

Simplified Approaches for the Risk Assessment of Non-Ductile Infilled RC Structures

Speaker:

Al Mouayed Bellah Nafeh – IUSS Pavia

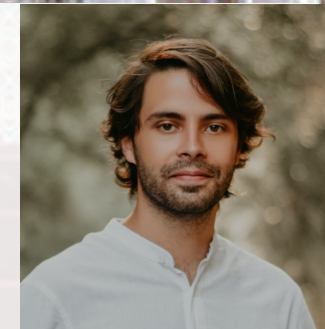
When:

12th October 2022 17:00 CET

Where:

Sala del Camino, Piazza della Vittoria 15, Pavia

<https://iusspavia.zoom.us/j/83114566728>



IUSS

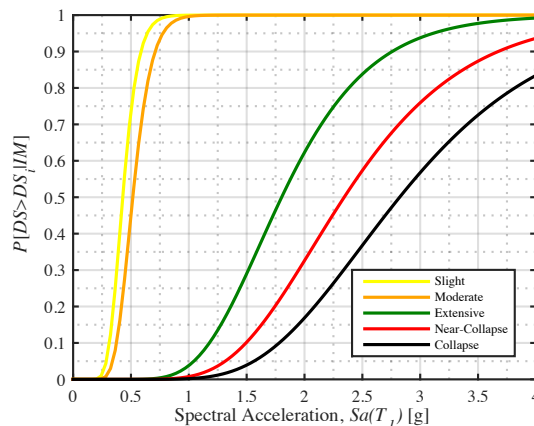
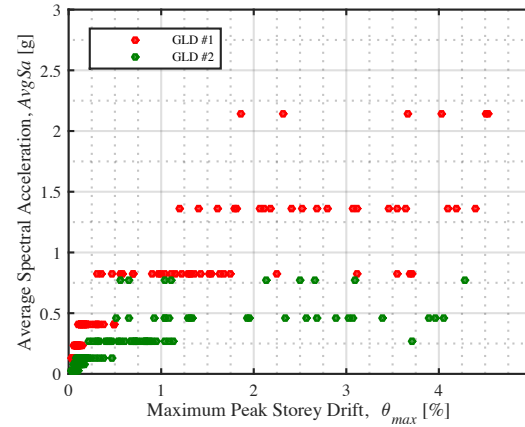
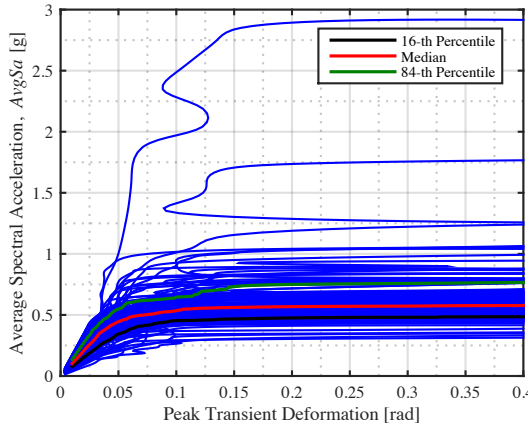
Scuola Universitaria Superiore Pavia

ROSE Centre

Centre for Training and Research
on Reduction of Seismic Risk

Web: www.iusspavia.it/rose Email: rose@iusspavia.it

Can we reduce the computational burden associated with time-consuming non-linear time-history procedures?



NATIONAL RESEARCH COUNCIL OF ITALY
ADVISORY COMMITTEE
ON TECHNICAL RECOMMENDATIONS FOR CONSTRUCTION

Guide
for the Probabilistic Assessment
of the Seismic Safety
of Existing Buildings



CNR-DT 212/2013

ROMA – CNR May 14th 2014

How to eliminate bias in the structural response to the excessive scaling of ground-motion records in incremental dynamic analysis?

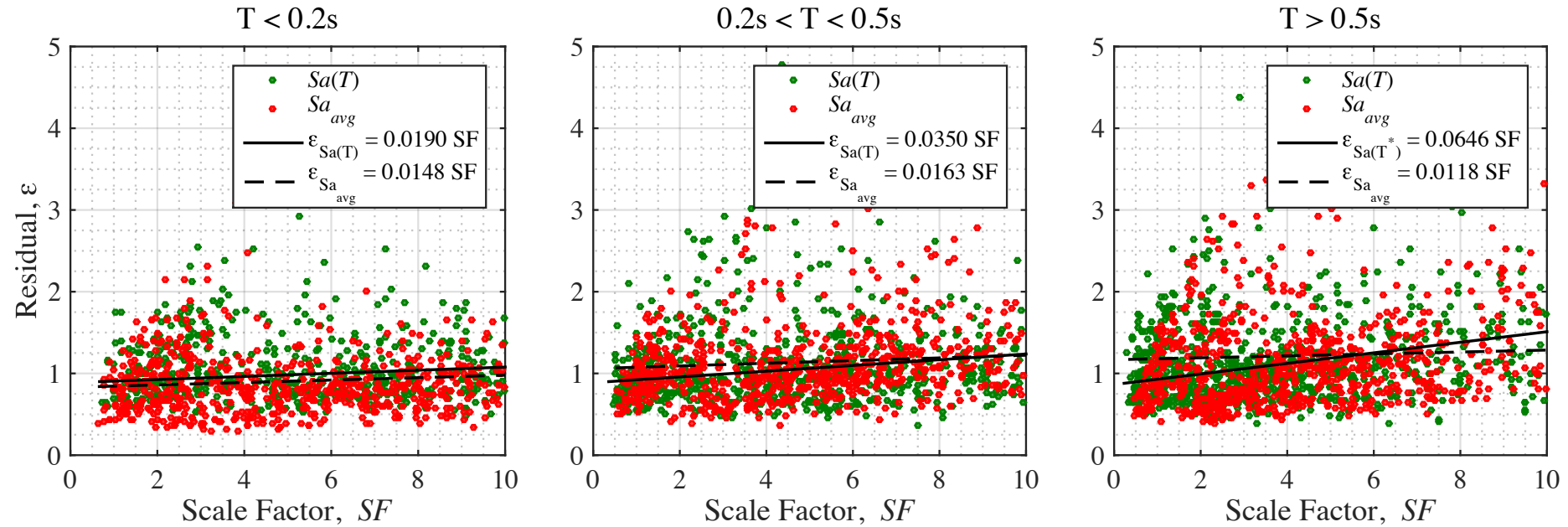
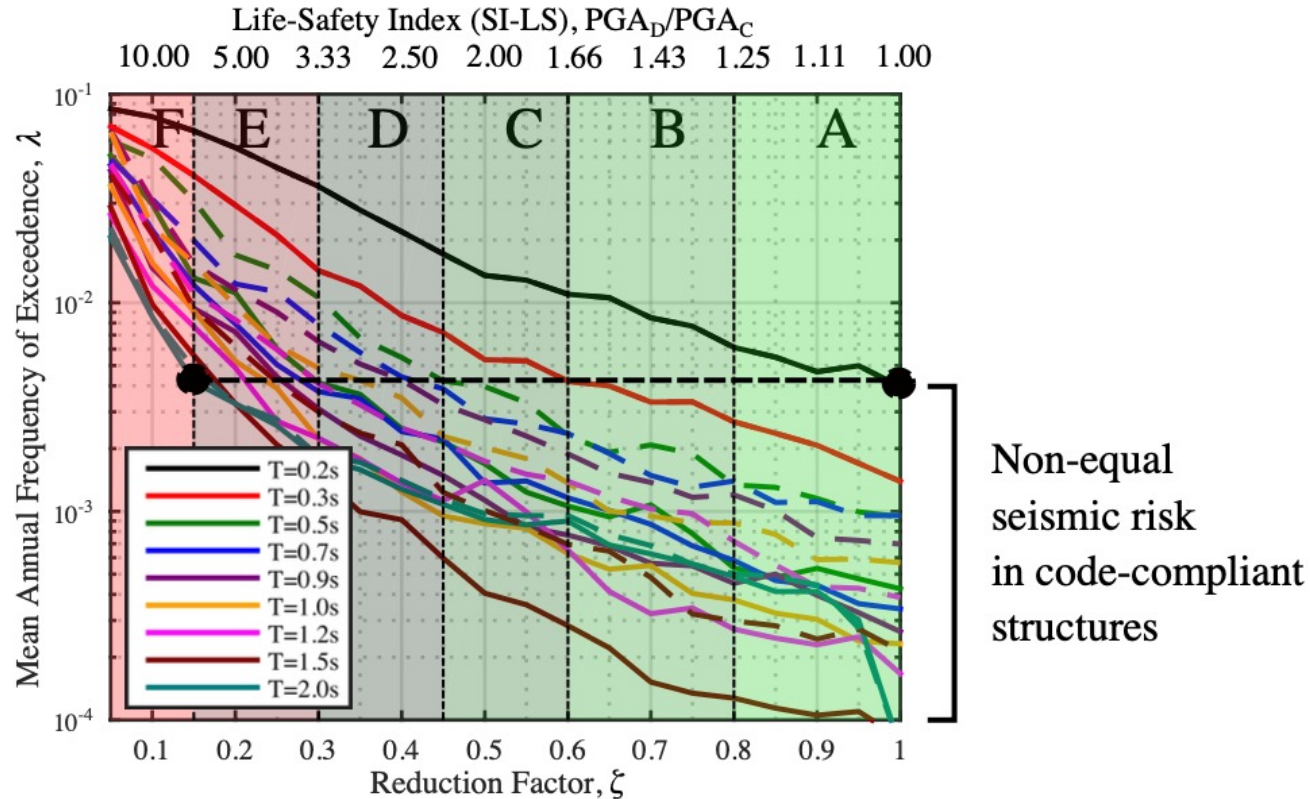


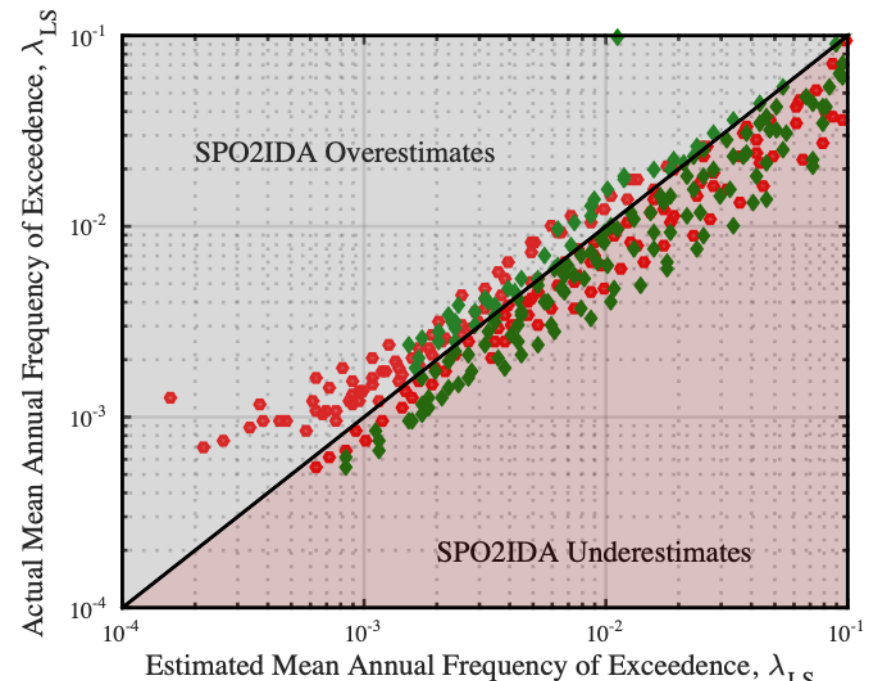
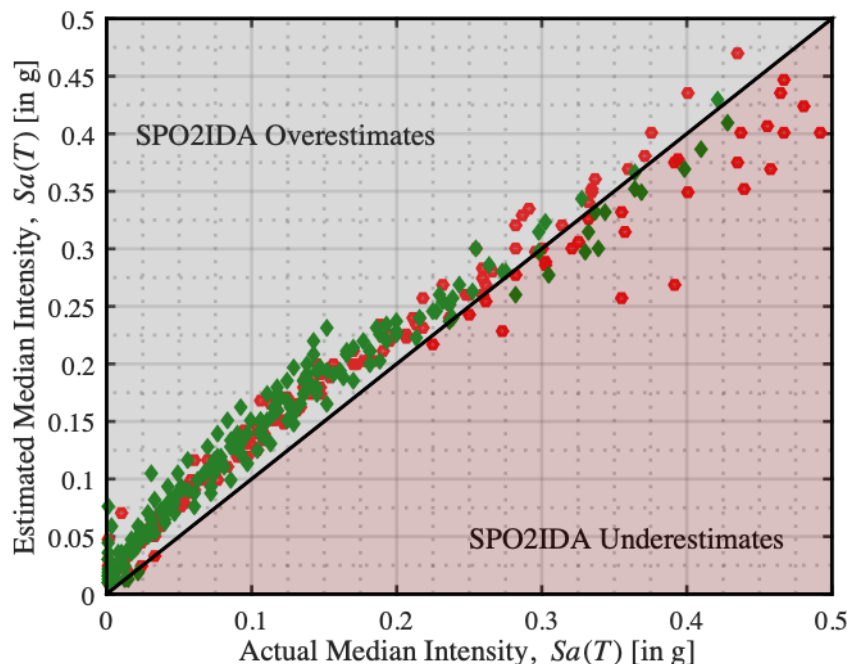
Illustration of the trend between the residual, ε , and the ground motion scale factor, SF, required to induce collapse for SDOF systems with low, moderate and high periods of vibration obtained from IDA.

Do current risk classification schemes communicate uniform risk estimates? What is the metric to be adopted for risk classification schemes of existing structures?



Non-uniformity of risk for SDOFs for both medium (solid lines) and high (dashed lines) ductility classes versus periods of oscillation, T , and strength modification factor, ξ

Do current risk classification schemes communicate uniform risk estimates? What is the metric to be adopted for risk classification schemes of existing structures?



Comparison of the median intensity and MAFE value estimated from SPO2IDA versus detailed analysis for both medium (green) and high (red) ductility classes



Development of a database for infilled RC archetype building numerical models

A.M.B, Nafeh, O'Reilly, G.J., *Unbiased simplified seismic fragility estimation of non-ductile infilled RC structures*, Soil Dynamics and Earthquake Engineering, Volume 157, 2022, 107253, ISSN 0267-7261, <https://doi.org/10.1016/j.soildyn.2022.107253>.

Identification of Design Space

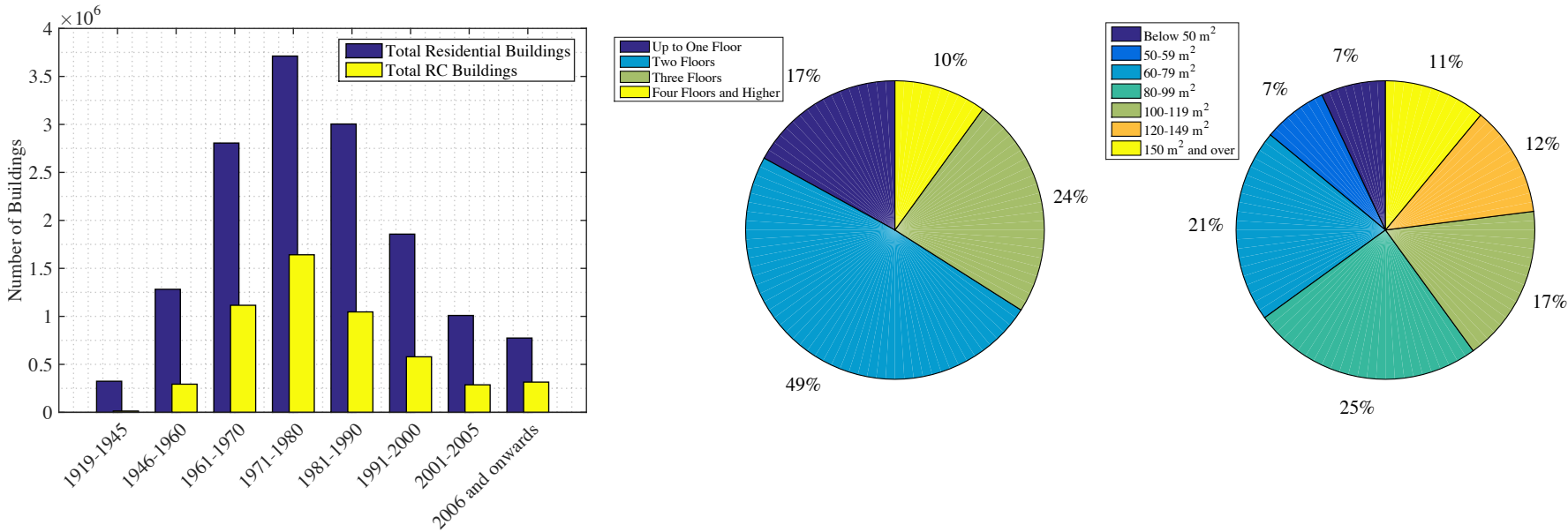
Archetype Design Consideration	Construction Era	Design Methodology	Design Considerations
Gravity-Load Design (GLD)	Pre-1970s	Gravity Loads + Allowable Stress Method (Royal Decree 2229/39)	<ul style="list-style-type: none"> • Frames spanning in one direction • Smooth rebars with low yield strength (Aq42, $\sigma_{all,s} \approx 140$ MPa) • Concrete with low compressive strength ($\sigma_{all,c} \approx 5$ MPa) • Poor transverse detailing and low shear reinforcement ratios • Inadequate detailing of beam-column joints
Sub-Standard Design (SSD)	1970s-1980s	Equivalent Lateral Force Method + Allowable Stress Method (L. 1086/71, DM 40/1975, DM 108/1986)	<ul style="list-style-type: none"> • Frames spanning in one (or both) directions • Deformed rebars with moderate yield strengths (FeB44k, $\sigma_{all,s} \approx 260$ MPa) • Concrete with moderate compressive strength ($\sigma_{all,c} \approx 7.5$ MPa) • No consideration for ductile detailing
High Seismic Design (HSD)	1990s (Before EC8 & Capacity-Based Design)	Response Spectrum Analysis	<ul style="list-style-type: none"> • Frames spanning in both directions • Deformed rebars with high yield strength ($\sigma \approx 430$ MPa) • Concrete with high compressive strength ($\sigma \approx 25$ MPa) • No mandatory capacity-based design or seismic detailing

Database of Archetype Buildings

ROSE Online Seminar

12th October 2022

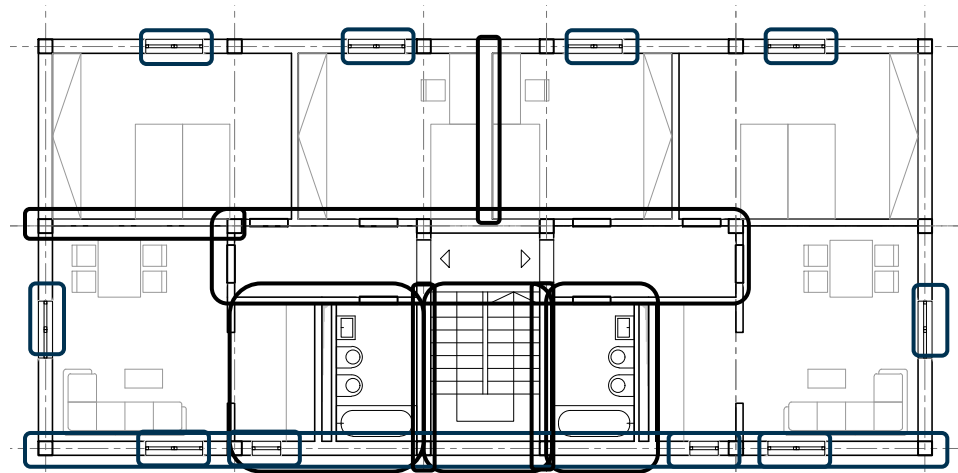
Identification of Key Building Characteristics



(left) Evolution of the Italian built environment; Percentage of dwellings disaggregated per surface area (right) and per total number of floors (center) [Extracted from ISTAT]

Identification of Key Architectural Considerations

- Expert architectural judgement (i.e. consultation with practitioners and review of past guidelines)
- Geometric configuration and architectural features selected to reflect the function and form of the Italian design space over different building periods, for example:
 - Narrow hallways and corridors in dwellings, generally 150 cm wide
 - Adjacent kitchens and bathrooms
 - Plumbing fixtures (e.g. bathtubs, sinks and bidets) installed based on optimized space allocation
 - Adequate separation of the day and night living spaces
 - Windows with widths in multiples of 45 or 60 cm
 - Staircase width not exceeding 3 m (i.e. wide enough to allow the passage of two people) and landings depth not exceeding 1.3 m
 - Double-leaf masonry infills for thermal and acoustic insulation and fire-retarding
 - 24 cm infill panels for perimeter walls of the façade
 - 30 cm infill panels for the separation of dwellings and encasing of the staircase
 - 80 mm single-leaf masonry infills for Internal partitioning and compartmentalization of the living space.

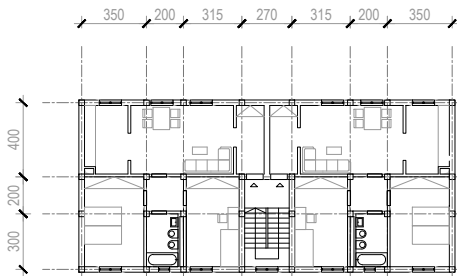


Database of Archetype Buildings

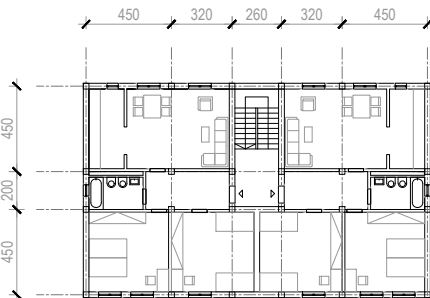
ROSE Online Seminar

12th October 2022

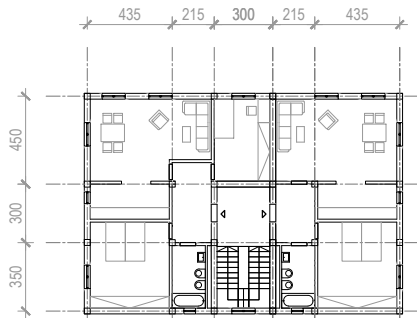
Identification of Key Architectural Considerations



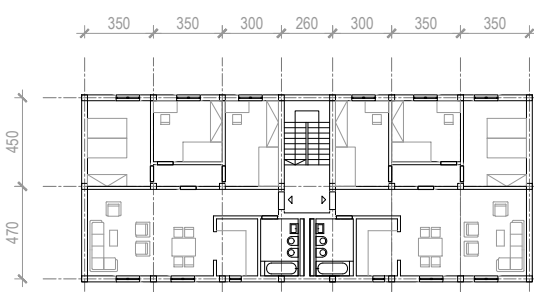
Archetype A



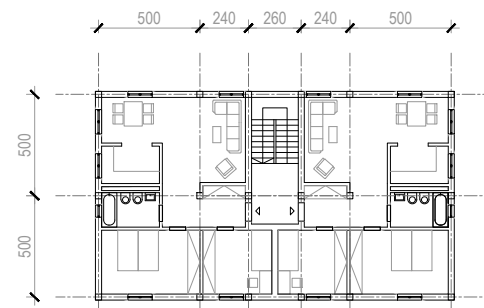
Archetype B



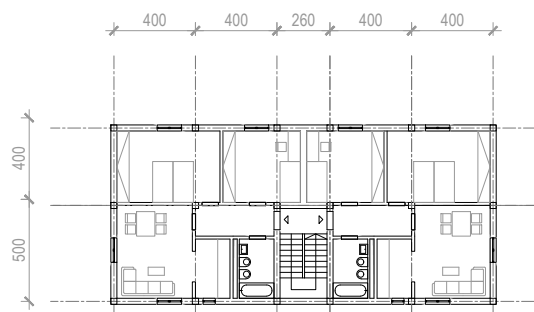
Archetype C



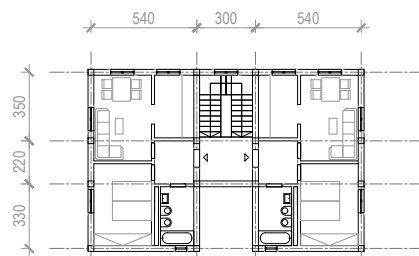
Archetype D



Archetype E

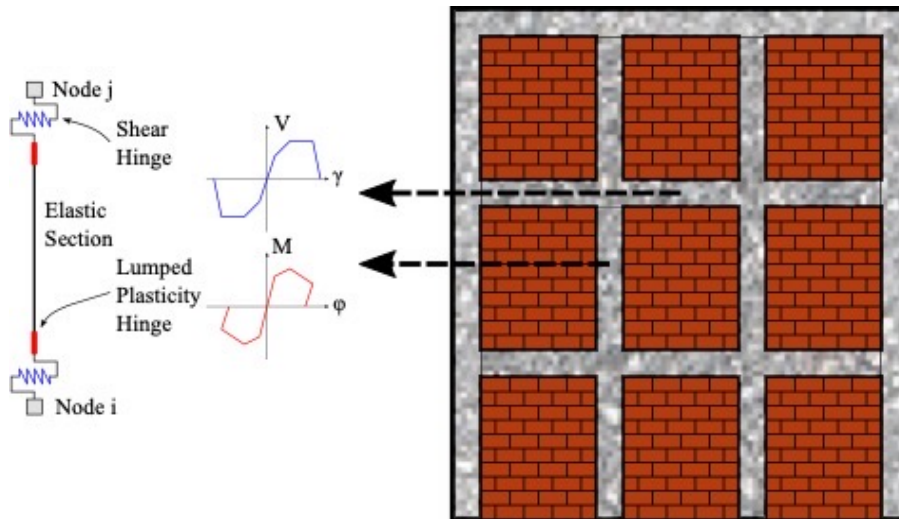


Archetype F



Archetype G

Numerical Modelling of Archetype Buildings (Beam-Column Elements)

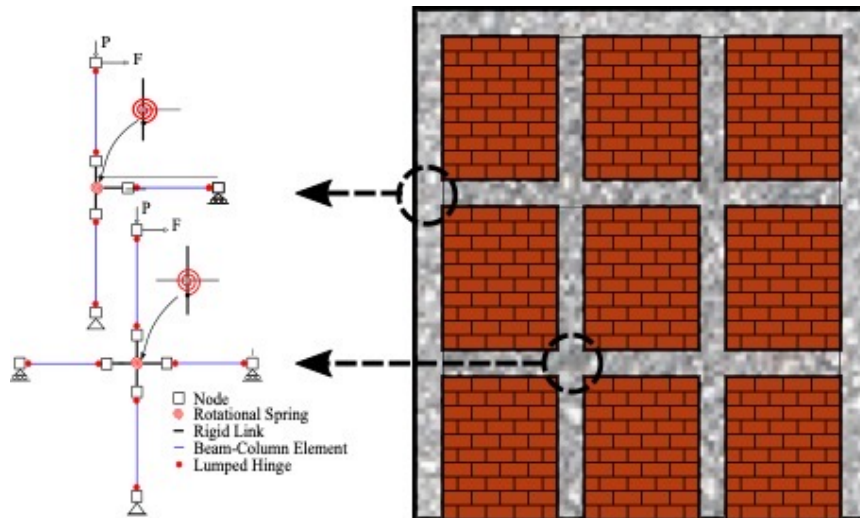


- “forceBeamColumn” elements with a finite plastic hinge length.
- “Pinching4” hysteretic material model based on the force-deformation relationships for non-conforming structures

Proposed beam-column element modelling that consists of a lumped hinge beam- column element to describe the flexural behaviour of the member together in series with an aggregated shear hinge that allows for the uncoupled shear response of the member to be accounted for.

- Verderame GM, Ricci P, De Risi MT, Del Gaudio C. Experimental Assessment and Numerical Modelling of Conforming and Non-Conforming RC Frames with and without Infills. *J Earthq Eng* 2019. <https://doi.org/10.1080/13632469.2019.1692098>.
- O'Reilly GJ, Sullivan TJ. Modeling Techniques for the Seismic Assessment of the Existing Italian RC Frame Structures. *J Earthq Eng* 2017;1–35. <https://doi.org/10.1080/13632469.2017.1360224>.

Numerical Modelling of Archetype Buildings (Beam-Column Joints)

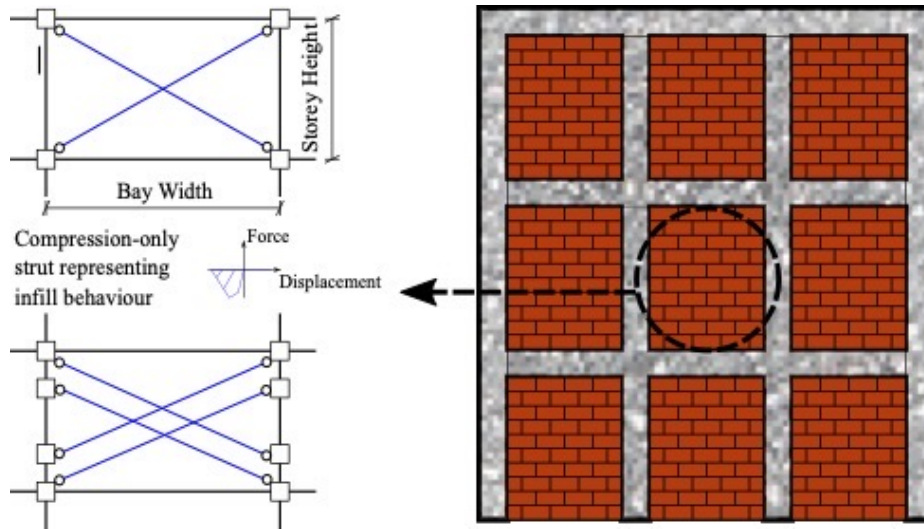


Proposed model layout for interior and exterior beam-column Joints using rotational springs linking the vertical and Horizontal rigid links in a "Scissors Models"

- zero-length elements using a “Hysteretic” model elements to capture both flexural and axial behaviour
- Rigid-links offsets and lumped rotational spring for the shear deformation of the joint region
- Limit states determined through experimental observations, expressed as a function of the concrete tensile strength

- O'Reilly GJ, Sullivan TJ. Modeling Techniques for the Seismic Assessment of the Existing Italian RC Frame Structures. *J Earthq Eng* 2017;1–35. <https://doi.org/10.1080/13632469.2017.1360224>.
- De Risi MT, Verderame GM. Experimental assessment and numerical modelling of exterior non-conforming beam-column joints with plain bars. *Eng Struct* 2017. <https://doi.org/10.1016/j.engstruct.2017.07.039>.

Numerical Modelling of Archetype Buildings (Masonry Infills)



- In-plane behaviour modelled using the equivalent strut approach
- Compression-only single/double strut models
- Further improvements foresee the inclusion of an IP-OOP interaction modelling

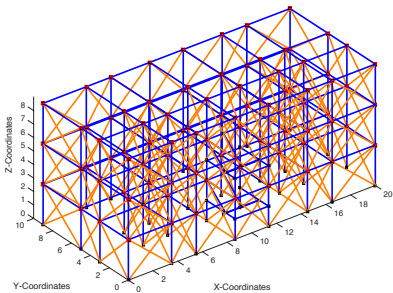
Various equivalent diagonal strut modelling approaches

- O'Reilly GJ, Sullivan TJ. Modeling Techniques for the Seismic Assessment of the Existing Italian RC Frame Structures. *J Earthq Eng* 2017;1–35. <https://doi.org/10.1080/13632469.2017.1360224>.
- Hak S, Morandi P, Magenes G, Sullivan TJ. Damage control for clay masonry infills in the design of RC frame structures. *J Earthq Eng* 2012;16:1 <https://doi.org/10.1080/13632469.2012.670575>.
- Crisafuli, F. J., Carr, A. J., Park, R. [2000] "Analytical Modelling of Infilled Frame Structures - A General Review," *Bulletin of the New Zealand Society for Earthquake Engineering*, Vol. 33, No. 1, pp. 30–47.
- Milanesi, R. R., Morandi, P., Hak, S., & Magenes, G. (2021). Experiment-based out-of-plane resistance of strong masonry infills for codified applications. *Engineering Structures*, 242, 112525.
- Morandi, P., Hak, S., Milanesi, R. R., & Magenes, G. (2022). In-plane/out-of-plane interaction of strong masonry infills: From cyclic tests to out-of-plane verifications. *Earthquake Engineering & Structural Dynamics*, 51(3), 648-672.

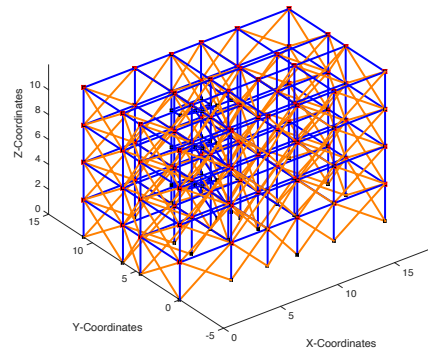
Database of Archetype Buildings

ROSE Online Seminar
12th October 2022

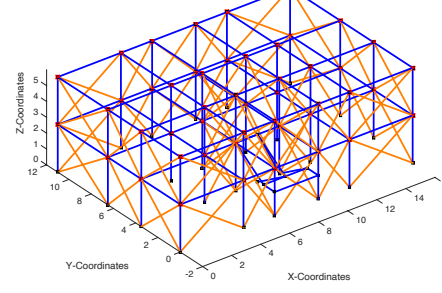
Numerical Modelling of Archetype Buildings



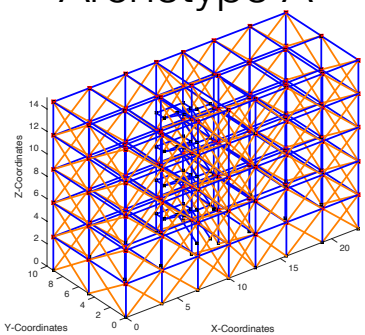
Archetype A



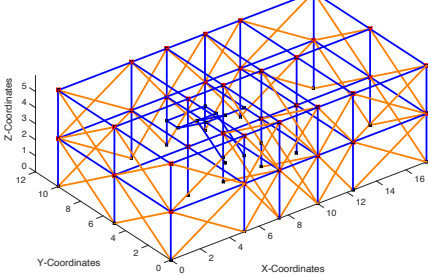
Archetype B



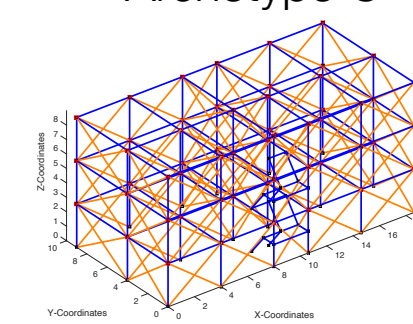
Archetype C



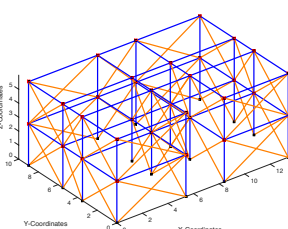
Archetype D



Archetype E



Archetype F



Archetype G

Conclusions

- Database of 315 representative archetype three-dimensional building numerical models in OpenSees (.tcl) was developed while OpenSeesPy is still under progress.
 - Typologies: Bare, Infilled, Pilotis RC Buildings
 - Stories: 2, 3, 4, 5 and 6 Storey Buildings
 - Repository contains also: Master files for running static (SPO) and cyclic (CPO) pushover analyses, incremental dynamic analysis (IDA) and multiple-stripe analysis (MSA)
- The database is available for download: <https://github.com/gerardjoreilly/Infilled-RC-Building-Database>



Response estimation tool (RET) for the seismic assessment of infilled RC buildings

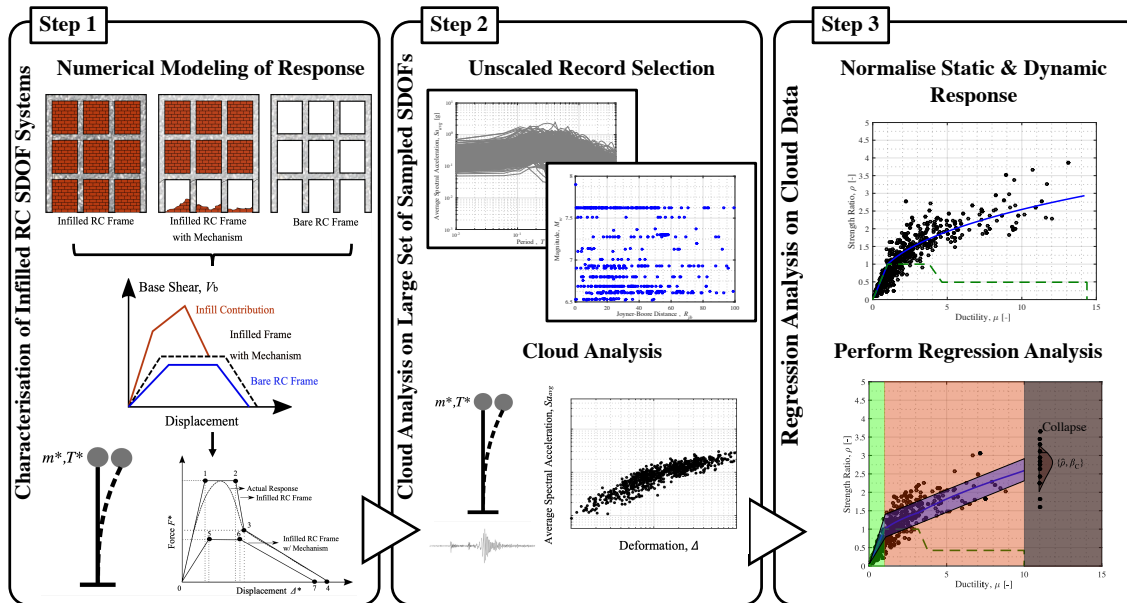
A.M.B, Nafeh, O'Reilly, G.J., *Unbiased simplified seismic fragility estimation of non-ductile infilled RC structures*, Soil Dynamics and Earthquake Engineering, Volume 157, 2022, 107253, ISSN 0267-7261, <https://doi.org/10.1016/j.soildyn.2022.107253>.

Simplified Response Estimation

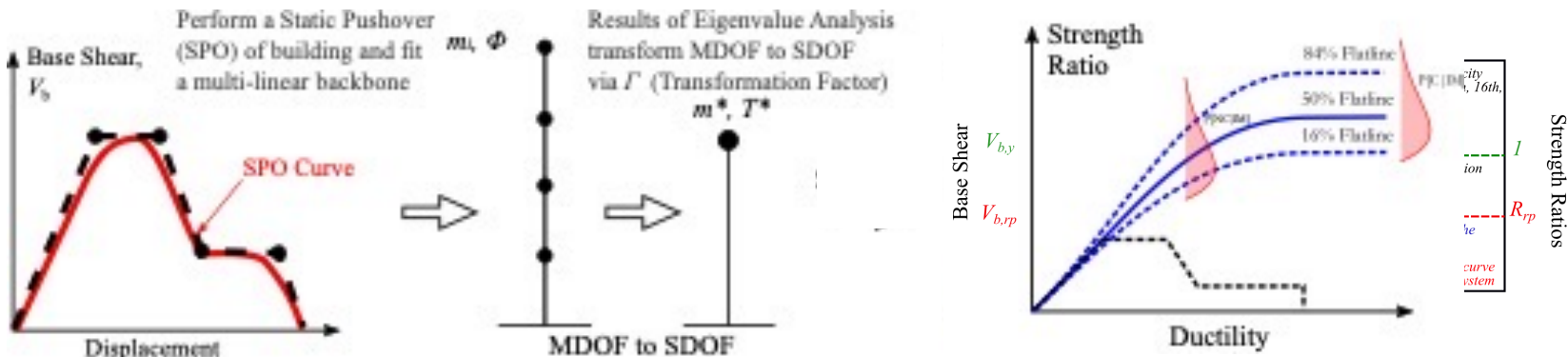
ROSE Online Seminar

12th October 2022

Development



Application

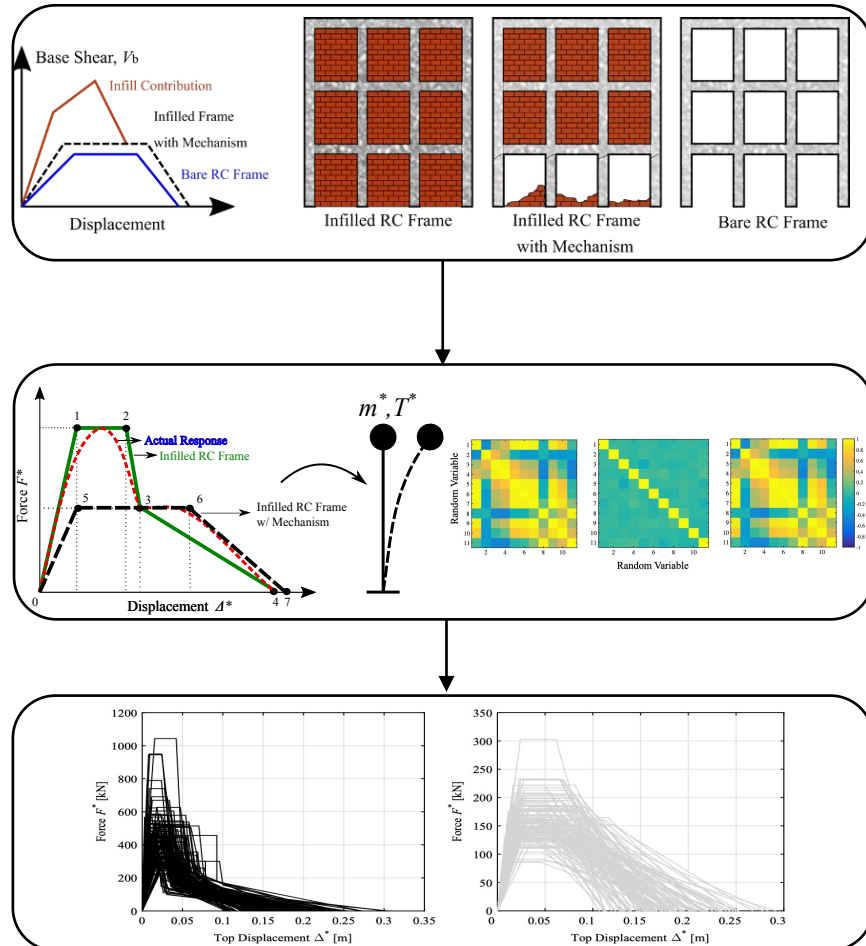


Simplified Response Estimation

ROSE Online Seminar

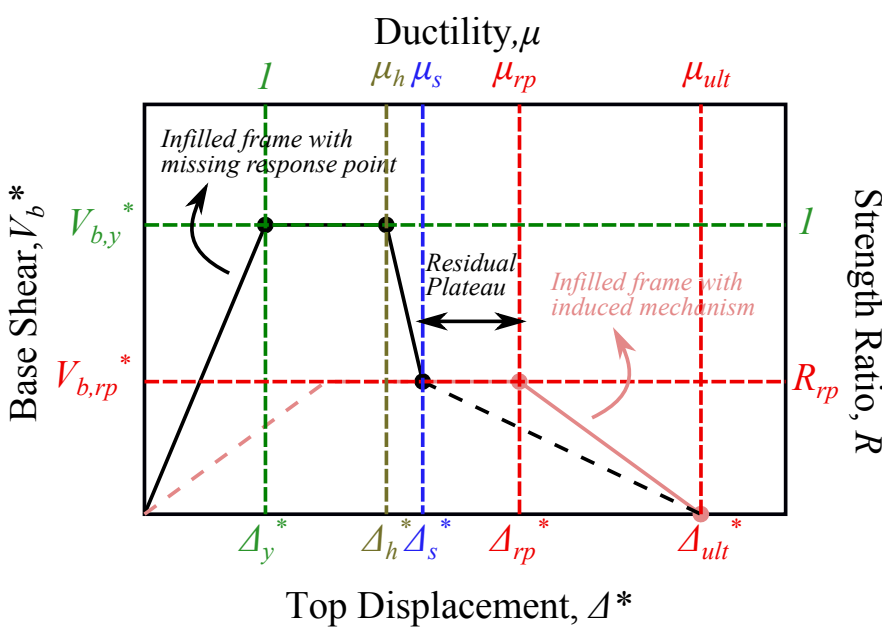
12th October 2022

Step 1(a): Characterisation and generation of representative equivalent SDOF (eSDOF) systems



- A population of case study frames were considered for the characterization of infilled RC frames behaviour
 - A suitable backbone definition, expressed in terms of base shear (V_b^*) - top deformation (Δ^*) was considered
 - Correlation-controlled Latin Hypercube sampling for the generation of random variables (i.e. backbone parameters) or random variables
 - Generation of eSDOF oscillators for the development of empirical strength-capacity relationships
- Nafeh AMB, O'Reilly GJ, Monteiro R. Simplified seismic assessment of infilled RC frame structures. *Bull Earthq Eng* 2020;18(4):1579–611. <https://doi.org/10.1007/s10518-019-00758-2>.

Step 1(b): Characterisation and generation of representative equivalent SDOF (eSDOF) systems



- For each sampled eSDOF, normalize the base shear (V_b^*) and top deformation (Δ^*) to obtain the static strength ratio (R) and ductility demand (μ)

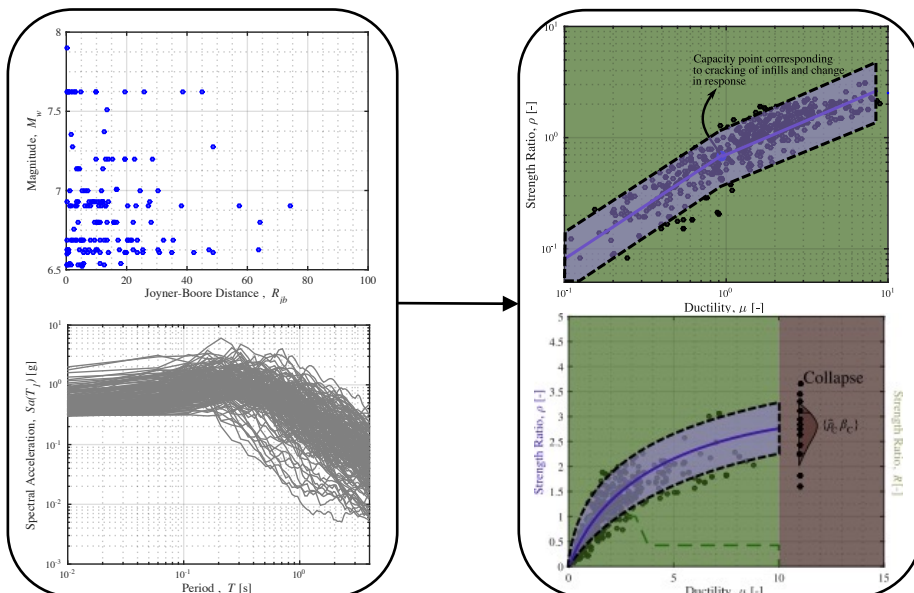
$$R = \frac{V_b^*}{V_{b,y}^*}; \mu = \frac{\Delta^*}{\Delta_y^*}$$

where V_b^* and $V_{b,y}^*$ are the base shear and yield nominal force of the SDOF system, respectively, and Δ^* and Δ_y^* are the corresponding displacement values

Simplified Response Estimation

ROSE Online Seminar
12th October 2022

Step 2: Perform cloud analysis on the representative set of ESDOF for the characterization of IM-EDP relationship



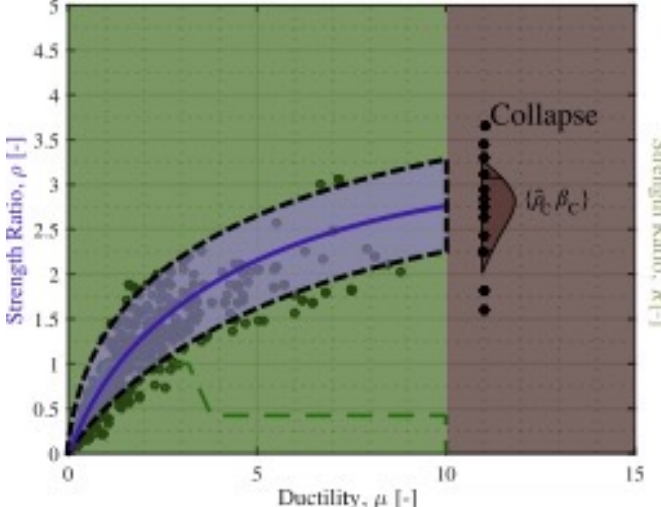
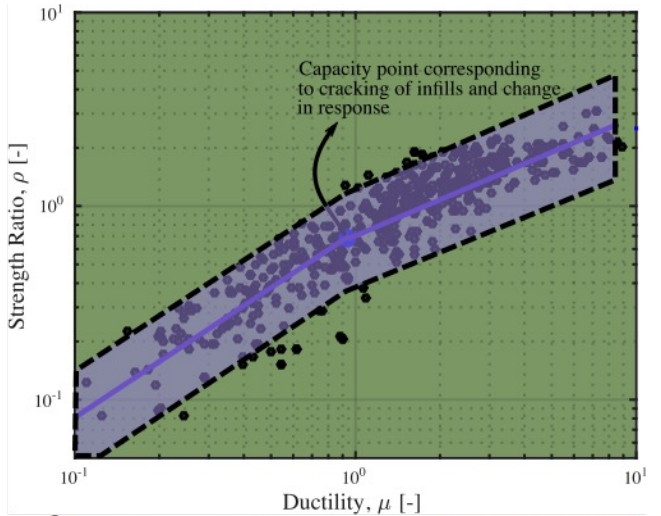
- Select a suitable set of unscaled ground motions to develop demand-intensity models
- Stratified selection of records was adopted to cover the entire range of structural response (EDP) where magnitude-distance bins are defined and n records were selected
- Cloud analysis was performed on each SDOF system and the IM (Sa_{avg}) and the structural response (Δ^*) was logged for each case

- Jalayer F, Ebrahimian H, Miano A, Manfredi G, Sezen H. Analytical fragility assessment using unscaled ground motion records. *Earthq Eng Struct Dynam* 2017; 46(15):2639–63. <https://doi.org/10.1002/eqe.2922>.
- Esteghamati MZ, Huang Q. An efficient stratified-based ground motion selection for cloud analysis. In: 13th International Conference on applications of statistics and probability in civil engineering. Seoul, South Korea: ICASP 2019; 2019.

Simplified Response Estimation

ROSE Online Seminar
12th October 2022

Step 3(a): Normalise the obtained deformation and IM levels following cloud analyses



- Normalise the deformation and intensity measure values obtained following cloud analyses, to determine the dynamic strength ratio (ρ) and ductility demand (μ)

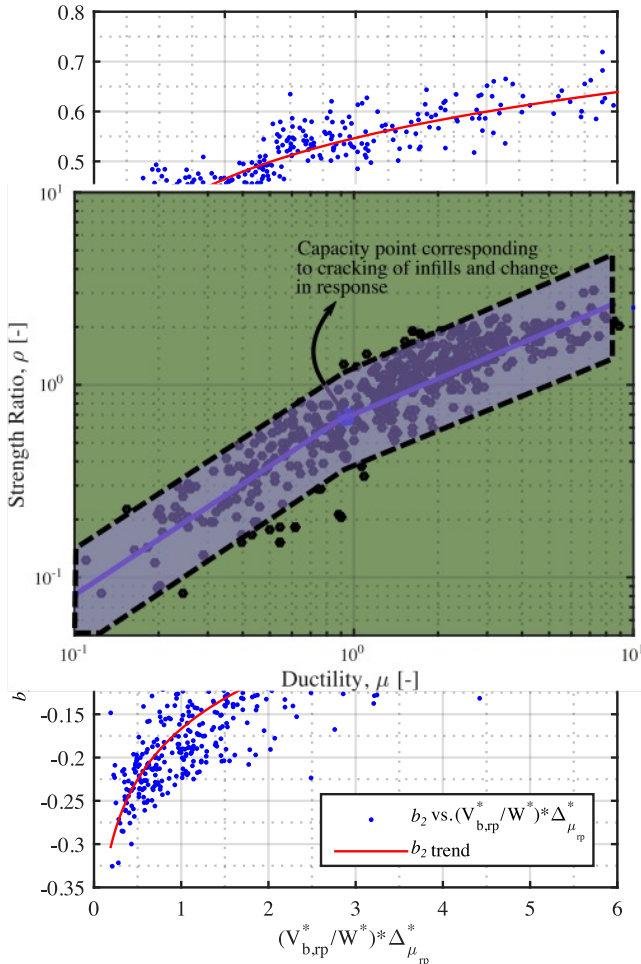
$$\rho = \frac{Sa_{avg}}{Sa_y}$$

$$Sa_y = \frac{4\pi^2 \Delta_y^*}{T^{*2} g} = \frac{V_{b,y}^*}{m^* g},$$

$$T^* = 2\pi \sqrt{m^* \frac{\Delta_y^*}{F_y^*}}$$

$$m^* = \sum m_i \Phi_i$$

Step 3(b): Two-step regression analyses on non-collapse cases



- A bilinear demand-intensity model is adopted which combines two linear models (i.e. elastic region and inelastic response)

$$\mu \leq 1, \hat{\rho}_{NC} = \exp(\ln(\mu) + b_2)$$

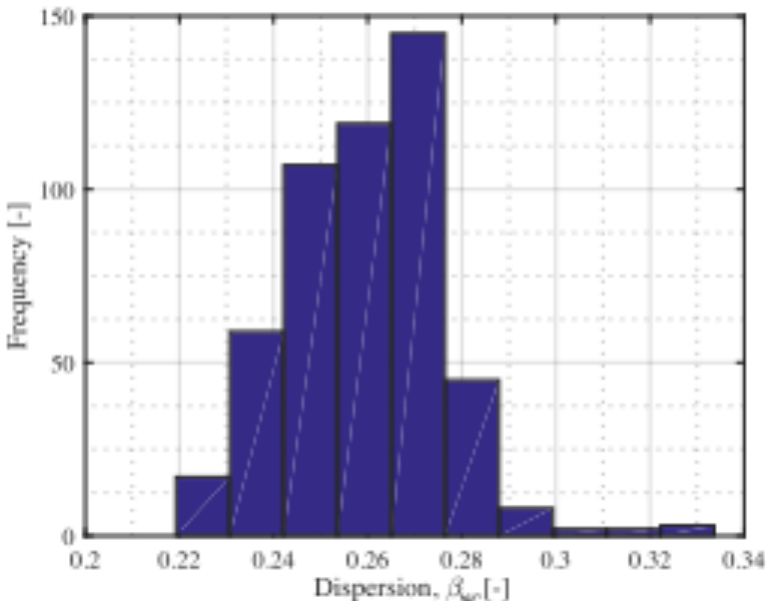
$$\mu > 1, \hat{\rho}_{NC} = \exp(a_2 \ln(\mu) + b_2)$$

- Two-step regression to relate the parameters of the fitted demand-intensity model (a_2, b_2) to the pushover response (T^* , base shear coefficient at yield and residual strength, ductility at residual strength and softening)

$$a_2 = 0.704 \left(\frac{T^*}{V_{b,y}^* / W^*} \right)^{0.1595} - 0.239;$$

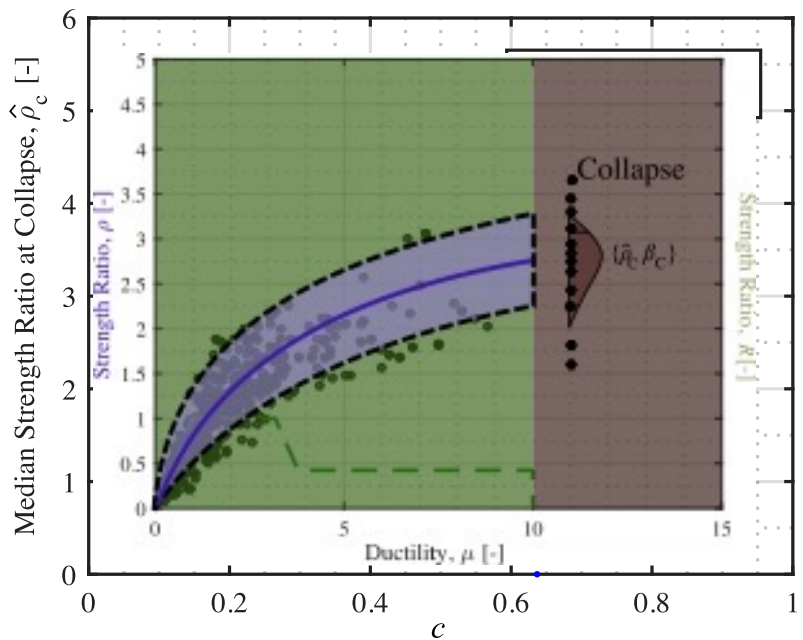
$$b_2 = 1.813 \left[\frac{V_{b,RP}^*}{W^*} (\mu_{RP} - \mu_s) \right]^{0.0473} - 1.98$$

Step 3(b): Two-step regression analyses on non-collapse cases



- The dispersion associated to $\hat{\rho}_{NC}$, denoted β_{NC} , refers to the standard deviation of the cloud data of the regressed demand-capacity model
- β_{NC} considers the record-to-record variability in the cloud analysis only
- $\beta_{NC} = 0.27$ was considered referring to the most frequently observed value of all cases

Step 3(c): Two-step regression analyses on collapse cases



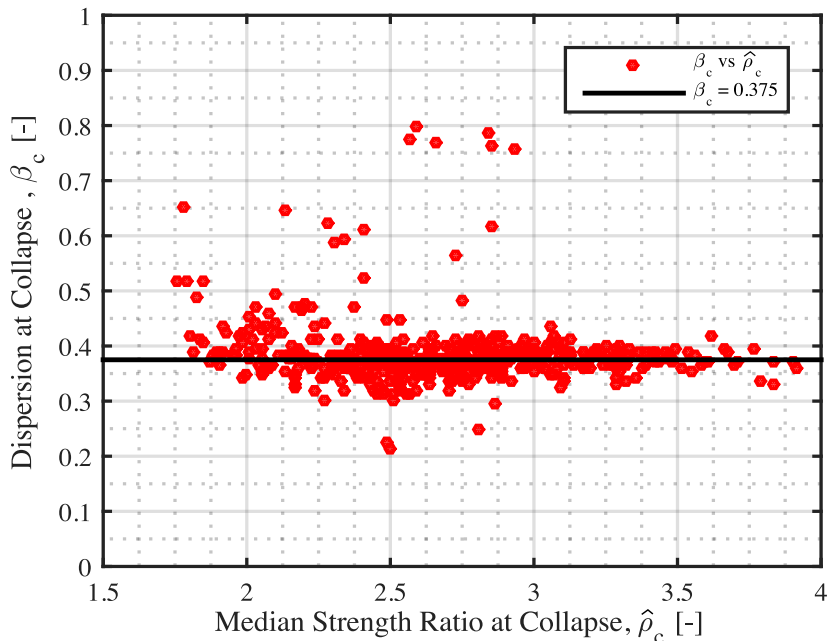
- A mathematical expression for the characterization of the median dynamic strength ratio was determined

$$\hat{\rho}_c = -1.62c + 3.32$$

- A two-step regression was carried out to relate the parameters of the fitted demand-intensity model to the pushover response (i.e. base shear coefficient at yield and residual strength, ductilities at residual strength, softening and ultimate)

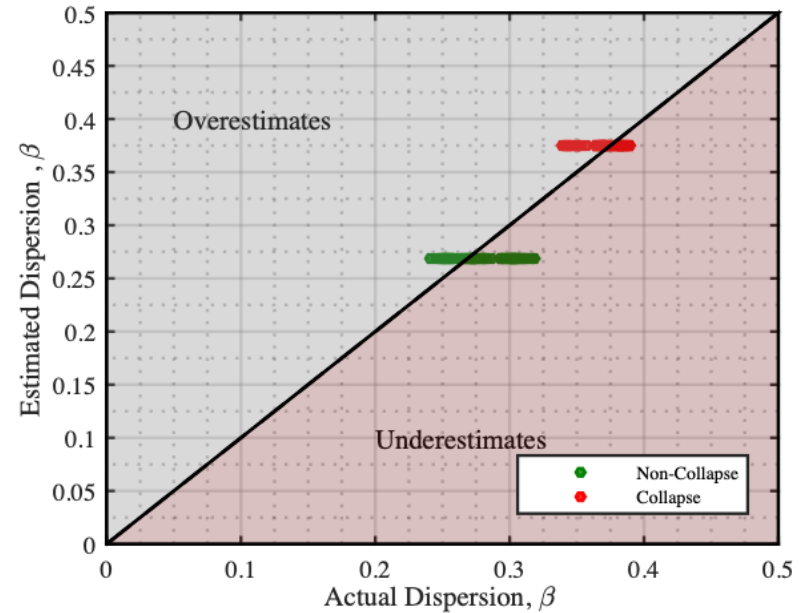
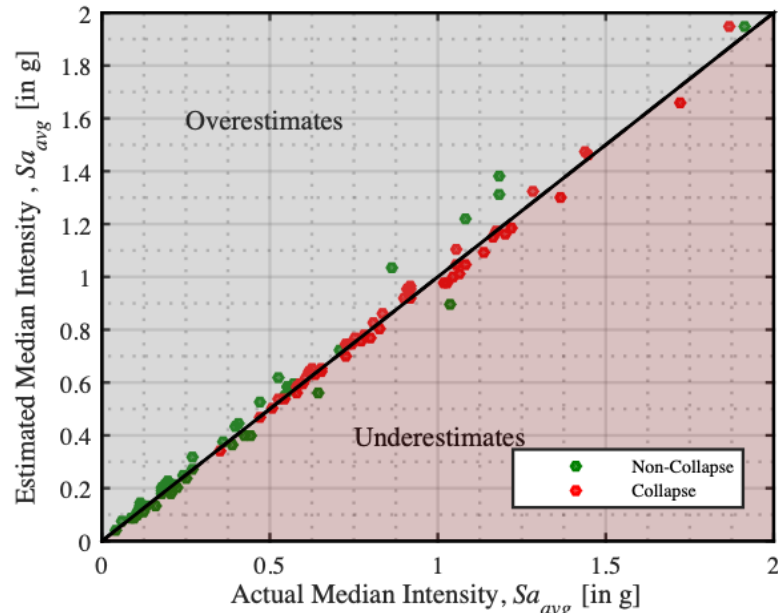
$$c = \left(1 - \left(\frac{V_{b,RP}^*}{V_{b,Y}^*} \right) \left(\frac{\mu_{RP} - \mu_s}{\mu_{ULT}} \right) \right)$$

Step 3(c): Two-step regression analyses on collapse cases



- The dispersion associated to $\hat{\rho}_c$, denoted β_c , refers to the standard deviation of the cloud data of the regressed demand-capacity model
- β_c considers the record-to-record variability in the cloud analysis only
- $\beta_c = 0.38$ was considered referring to the best fit value observed corresponding to the trend with respect to the median collapse intensities

Validation of results on SDOF oscillators



Comparison of the estimated (using proposed simplified approach) vs actual (using cloud analysis) median intensities corresponding to the non-collapsing performance limit of 1.0% top drift and collapse given in terms of Sa_{avg} and their respective dispersions.

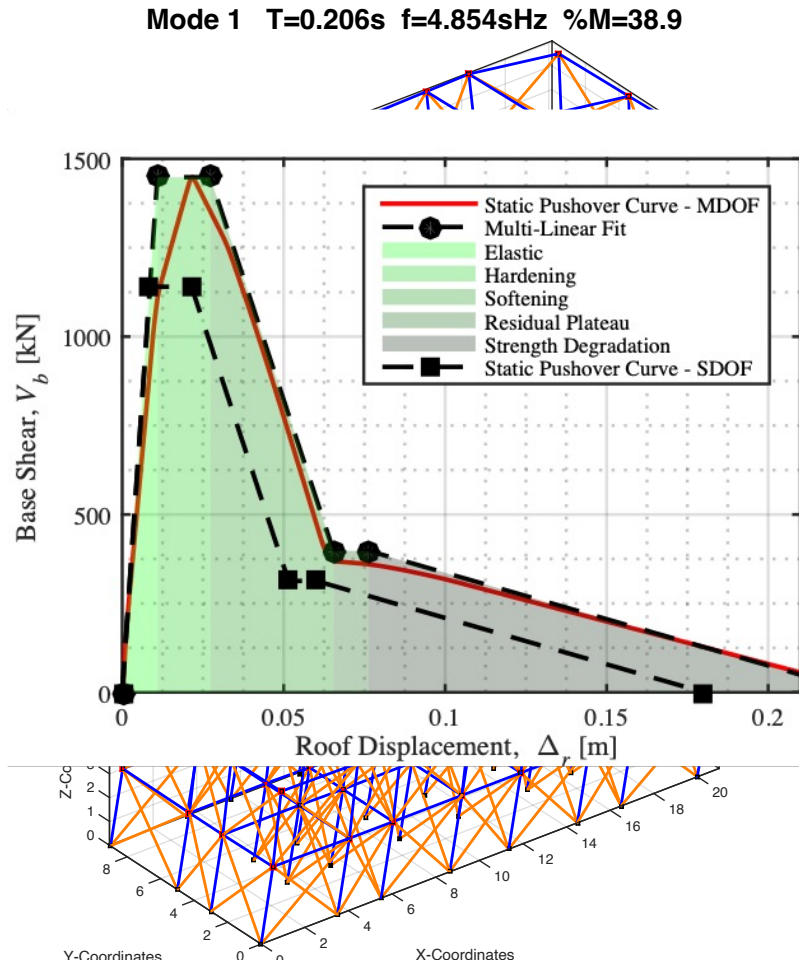
Simplified Response Estimation

ROSE Online Seminar

12th October 2022

Application of the Response Estimation Tool

- a. Build a sufficiently detailed numerical model of the structure under consideration that accounts for all possible inelastic mechanisms and potential failure modes expected in the structure;
- b. Perform an eigenvalue analysis to extract the first-mode shape ordinates ϕ , and identify the seismic mass m , at each floor level i .
- c. Perform a non-linear static pushover analysis in both principal directions of the MDOF structure to obtain the base shear versus roof displacement data, F and Δ , respectively.
- d. Fit a multi-linear backbone model to the MDOF's non-linear static pushover curves in both directions, which adequately captures the onset and end-point of each response branch

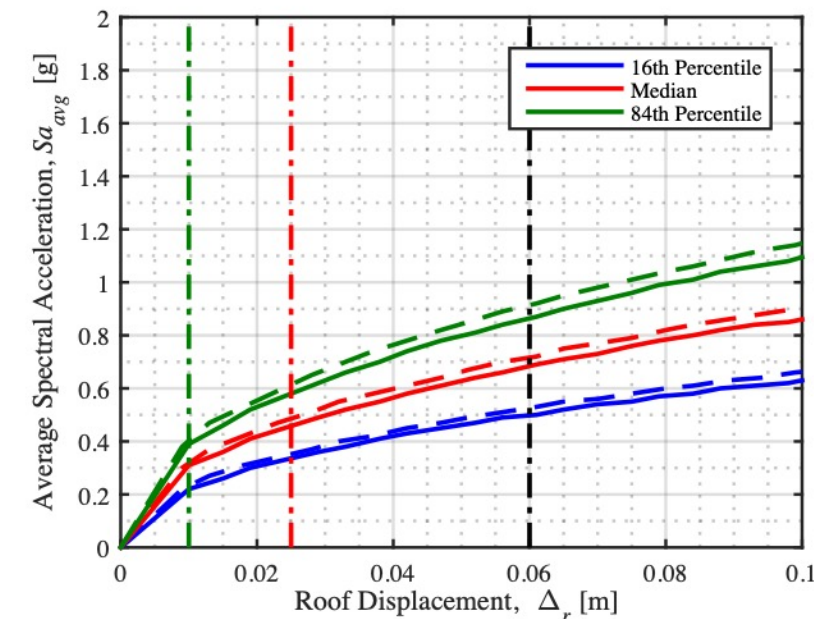


Application of the Response Estimation Tool

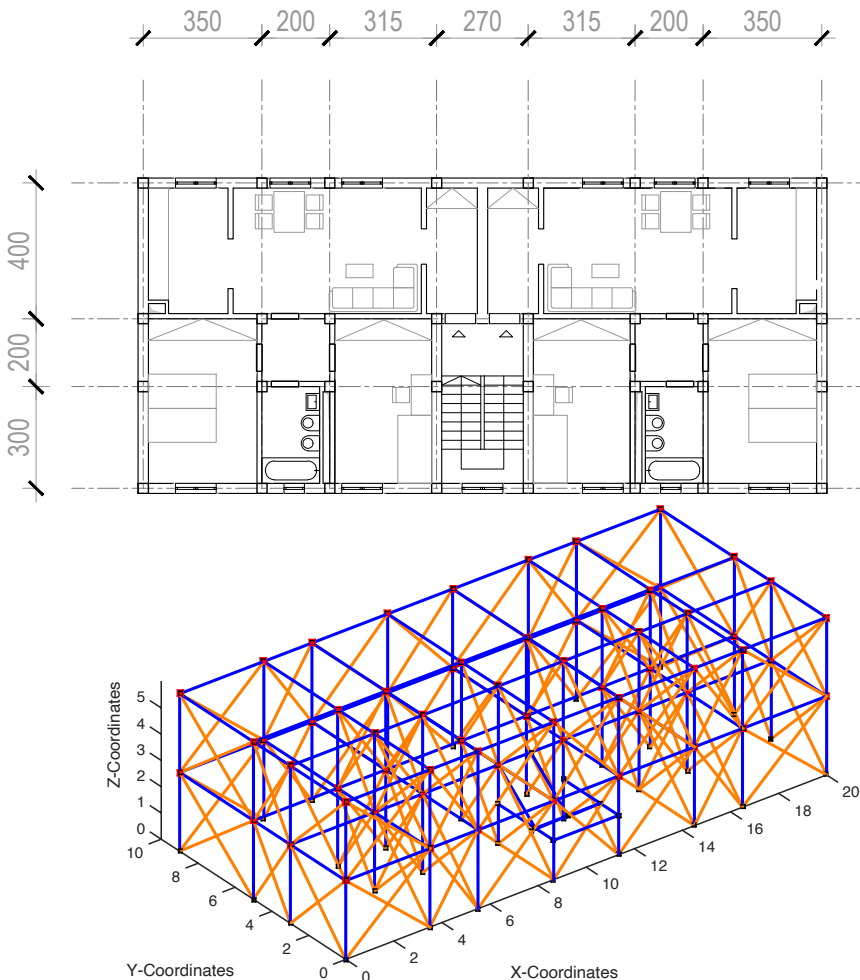
- e. Identify the LS criteria to be checked from either code-based demand thresholds, or other ad-hoc definitions, and mark them on both pushover curves.
- f. Using the response evaluation tool, the seismic demand-intensity model is calculated for the structure's equivalent SDOF in both directions. It is expressed in terms of a dynamic strength ratio, ρ , and global ductility, μ . the corresponding median intensity of the MDOF system is then determined as such:

$$\widehat{Sa}_{avg} = \rho Sa_y^* \Gamma$$

$$\Gamma = \frac{\sum m_i \Phi_i}{\sum m_i \Phi_i^2}$$

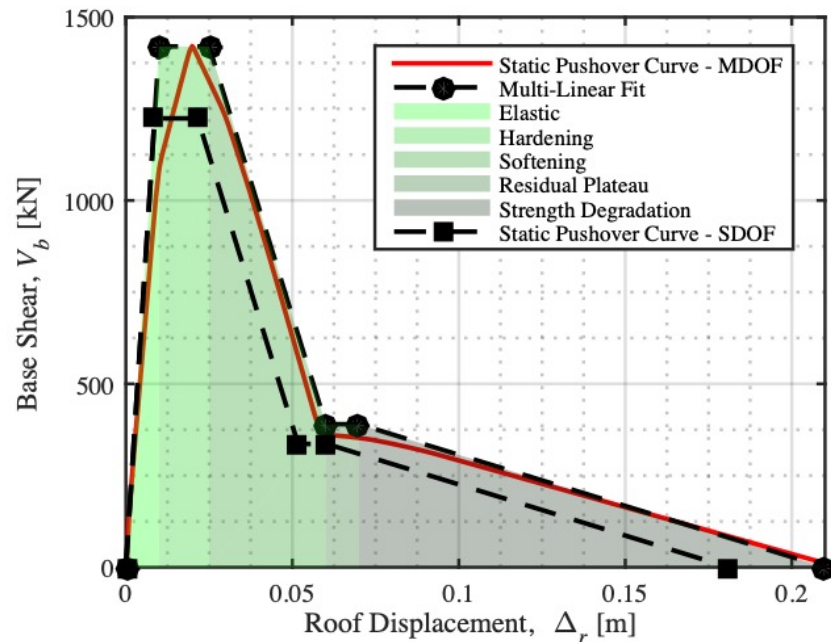
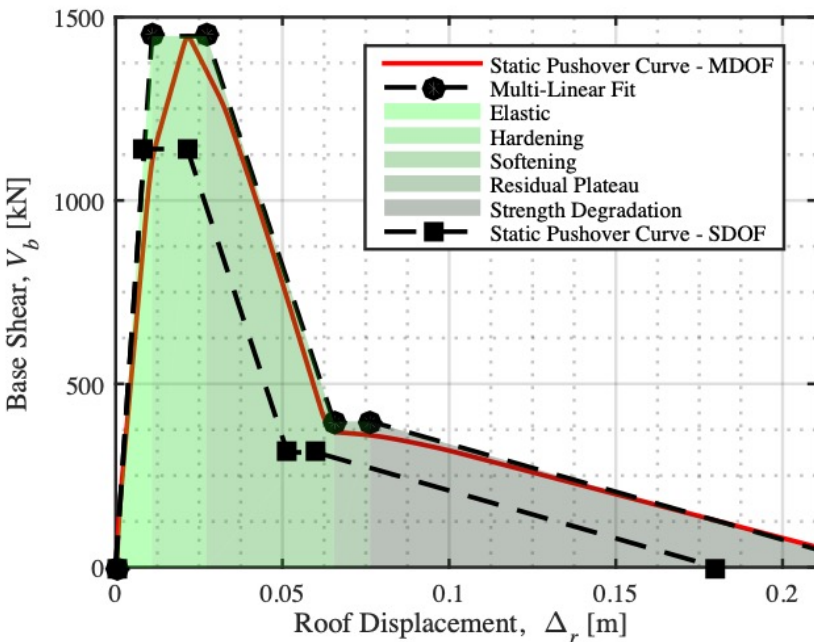


Example Application



- Design Method: Allowable Stress Method (Pre-1970s)
- Column Section: 20x20 cm
- Column Reinforcement Ratio: 0.89%
- Beam Section: 50x30 cm
- Beam Longitudinal Reinforcement Ratio: 0.21-0.31%
- Beam Transverse Reinforcement: $\Phi 6$ @ 150-200 mm
- Concrete Allowable Stress: 5 MPa
- Steel Rebars Allowable Stress: 140 MPa (Type Aq42)

Example Application



Non-linear static pushover curves for the X-direction (left) and Y-direction (right) showing base shear and the roof displacement and the multi-linear fits to compute the equivalent SDOF properties

Example Application

Floor	Mass, m_i [Tonnes]	First-Mode Shape $\Phi_i [-]$	Effective Mass, m^*	Transformation Factor, $\Gamma [-]$	Period, T^* [s]	Yield Spectral Acceleration, $Sa_y [g]$
0 (base)	-	-	340.64 (338.49)	1.18 (1.16)	0.33 (0.24)	0.37 (0.63)
1	215 (215)	0.58 (0.57)				
2 (roof)	215 (215)	1.00 (1.00)				

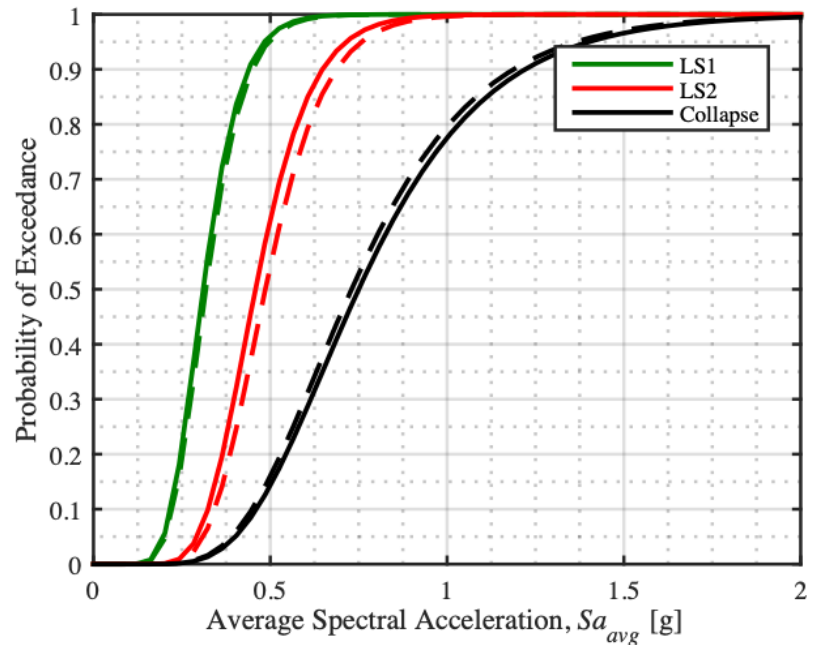
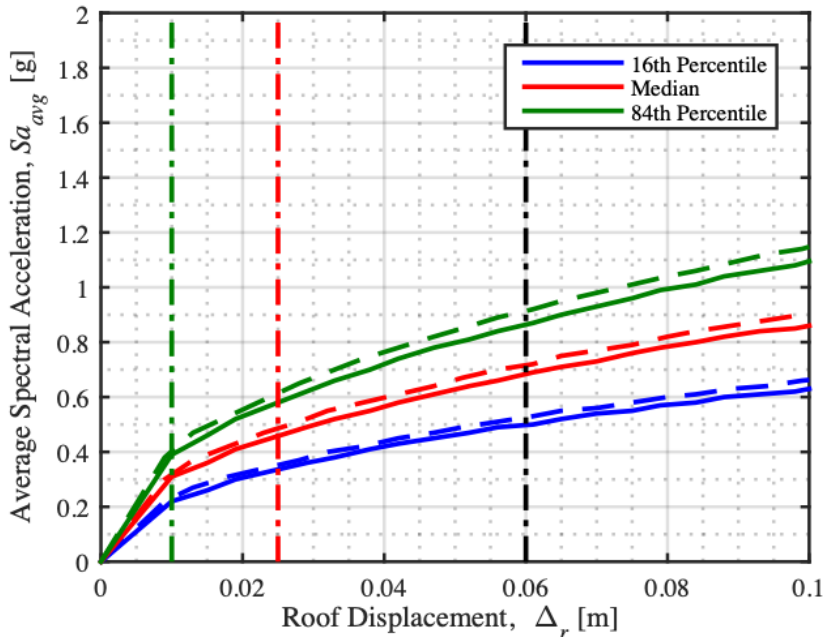
Eigenvalue analysis and the equivalent SDOF parameters in the two principal directions X and Y, where the latter values are denoted by the parentheses

Simplified Response Estimation

ROSE Online Seminar

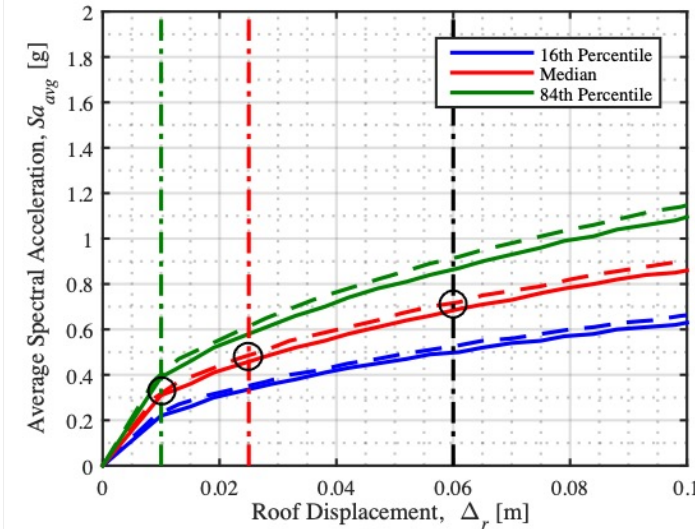
12th October 2022

Example Application



(left) Demand-capacity curves obtained using the response evaluation tool, illustrating the median response and quantiles (16th, 84th) corresponding to the estimated average spectral acceleration intensity against the roof displacement of the MDOF system;
(right) fragility curves corresponding to the two LSSs. Solid and dashed lines denote the X and Y directions, respectively. Vertical lines correspond to the limit-state thresholds

Example Application



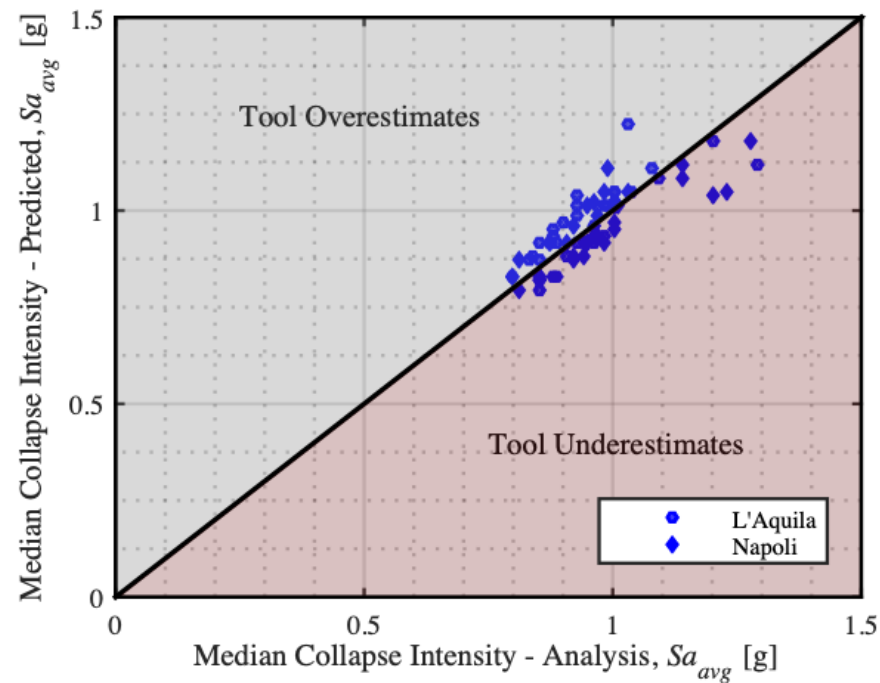
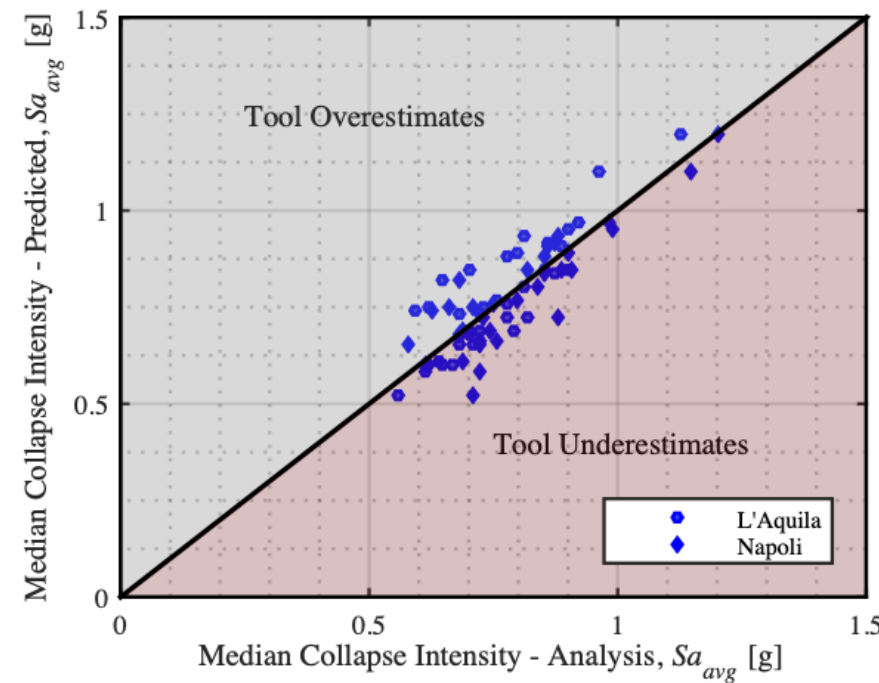
- $\widehat{Sa}_{avg|NC,X,LS1(D>0.01m)} = \hat{\rho}_{NC,X,LS1} Sa_{y,X}^* \Gamma_X = (0.71)(0.37g)(1.18) = 0.31g$
- $\widehat{Sa}_{avg|NC,X,LS2(D>0.01m)} = \hat{\rho}_{NC,X,LS2} Sa_{y,X}^* \Gamma_X = (1.05)(0.37g)(1.18) = 0.46g$
 - $\beta_{NC} = 0.27$
 - $\widehat{Sa}_{avg|C,X} = \hat{\rho}_{C,X,LS1} Sa_{y,X}^* \Gamma_X = (1.72)(0.37g)(1.18) = 0.75g$
 - $\widehat{Sa}_{avg|C,Y} = \hat{\rho}_{C,Y,LS2} Sa_{y,X}^* \Gamma_Y = (0.99)(0.37g)(1.16) = 0.72g$
 - $\beta_C = 0.38$

Simplified Response Estimation

ROSE Online Seminar

12th October 2022

Validation of results on case study building population



Comparison of the median collapse intensity obtained from traditional analysis (MSA) considering the case study sites and the estimated intensities from the response evaluation tool (left: GLD, right: SSD).

Conclusions

- A simplified seismic assessment approach based on non-linear static analysis (i.e. pushover) to estimate the capacity of non-ductile infilled RC frame buildings has been presented and built into a simplified tool, providing ease of applicability for future users
- The cloud analysis performed in the development phase of the proposed approach addresses the issue of potentially biased response predictions introduced through high ground motion scaling factors and poor choice of intensity measure encountered when following existing methods
- The capability of the tool in accurately quantifying the collapse capacity renders it a potential improvement to be implemented in risk classification guidelines such as Sismabonus in Italy, specifically for the infilled RC typology
- The tool is available for download in spreadsheet format:
<https://github.com/gerardjoreilly/Infilled-RC-Building-Response-Estimation>



Simplified seismic risk estimation of infilled RC frame buildings for code-based applications

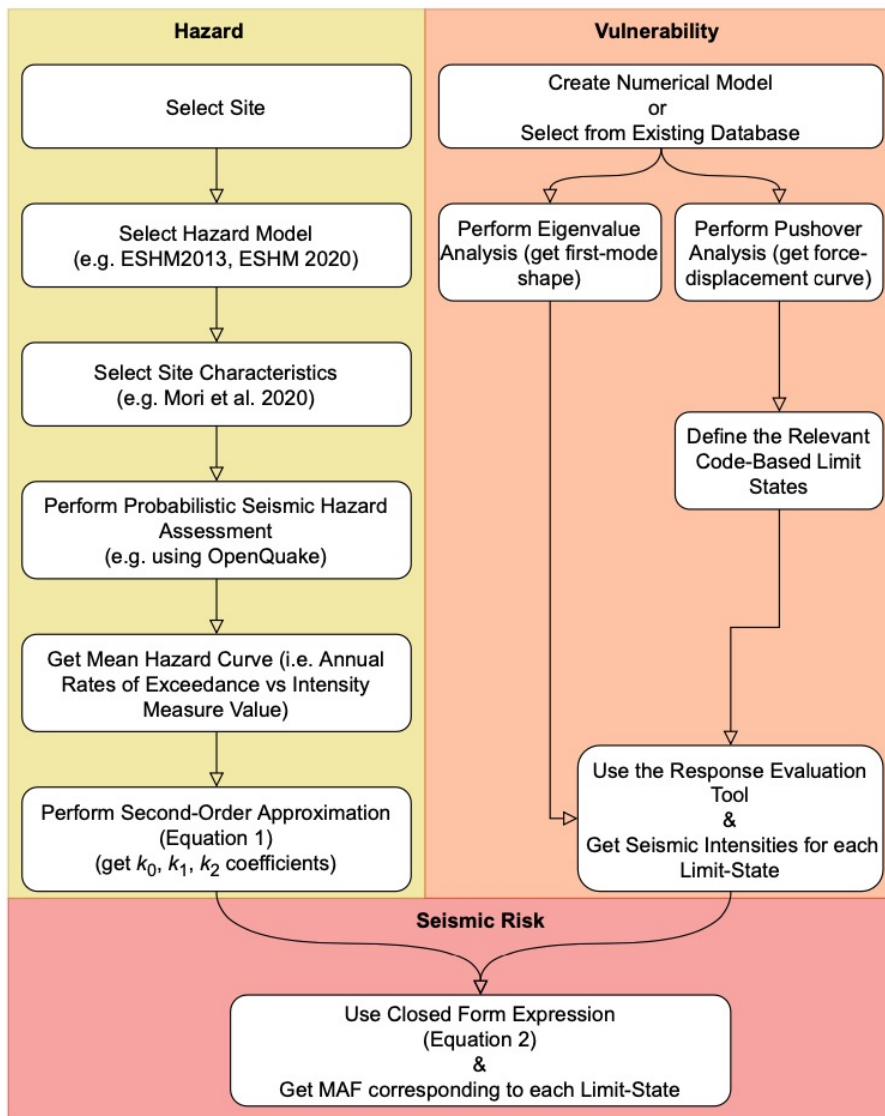
A.M.B, Nafeh, O'Reilly, G.J., *Simplified pushover-based seismic risk assessment methodology for existing infilled RC frame structures*, *Bulletin of Earthquake Engineering*, 2022 (Under Review)

A.M.B, Nafeh, O'Reilly, G.J., *Simplified Seismic risk assessment of infilled RC frame buildings*, *Proceedings of the 3rd European Conference on Earthquake Engineering and Seismology*, 2022, Bucharest, Romania.

Simplified Risk Estimation

ROSE Online Seminar

12th October 2022

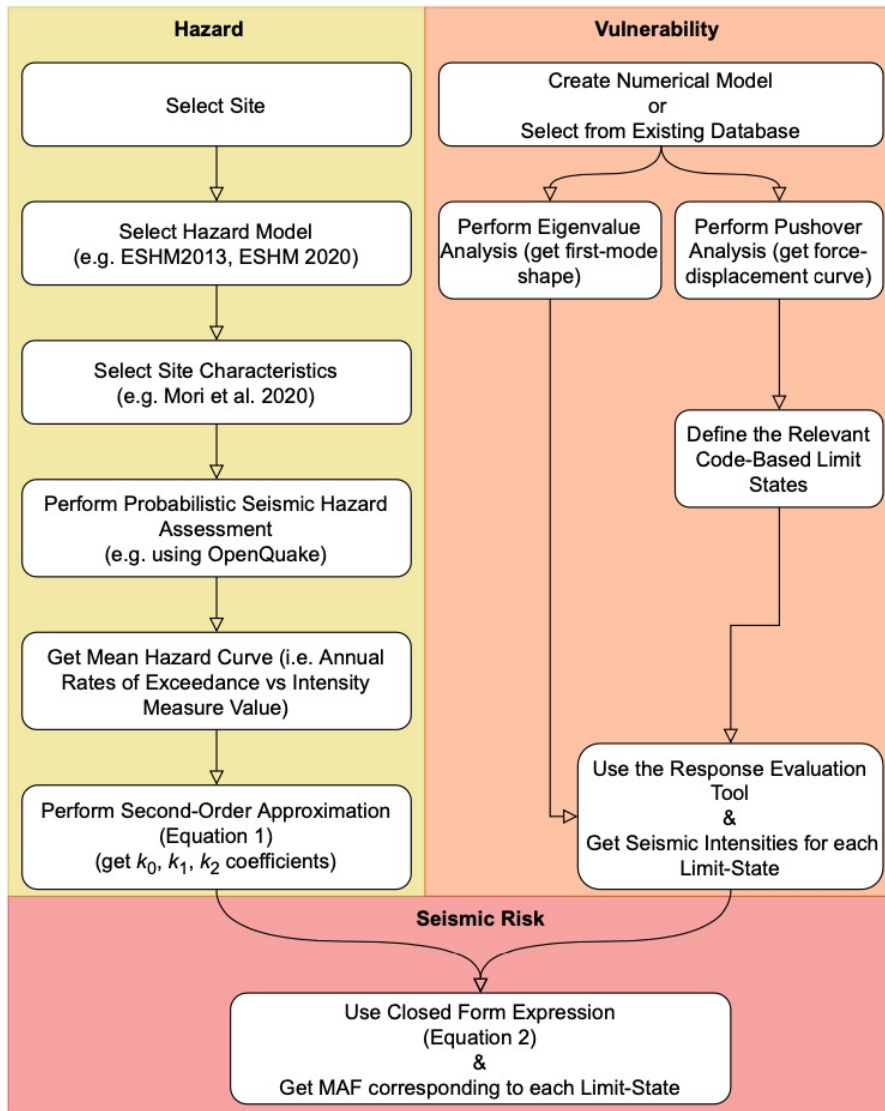


- A relatively fast and simple method (PB-Risk) for the seismic risk estimation of non-ductile infilled RC structures
- Integration of high-fidelity mathematical expression and statistical models for the characterisation of hazard and vulnerability
- Intensity-based closed-form solution (Vamvatsikos, 2013) to the risk integral for the derivation of risk expressed in terms of the mean annual frequency of exceedance

Simplified Risk Estimation

ROSE Online Seminar

12th October 2022



Hazard

1. Perform probabilistic seismic hazard assessment at the location of interest and get mean hazard curves
2. Fit second-order polynomial to mean hazard and obtain fit coefficients (k_0 , k_1 , k_2)

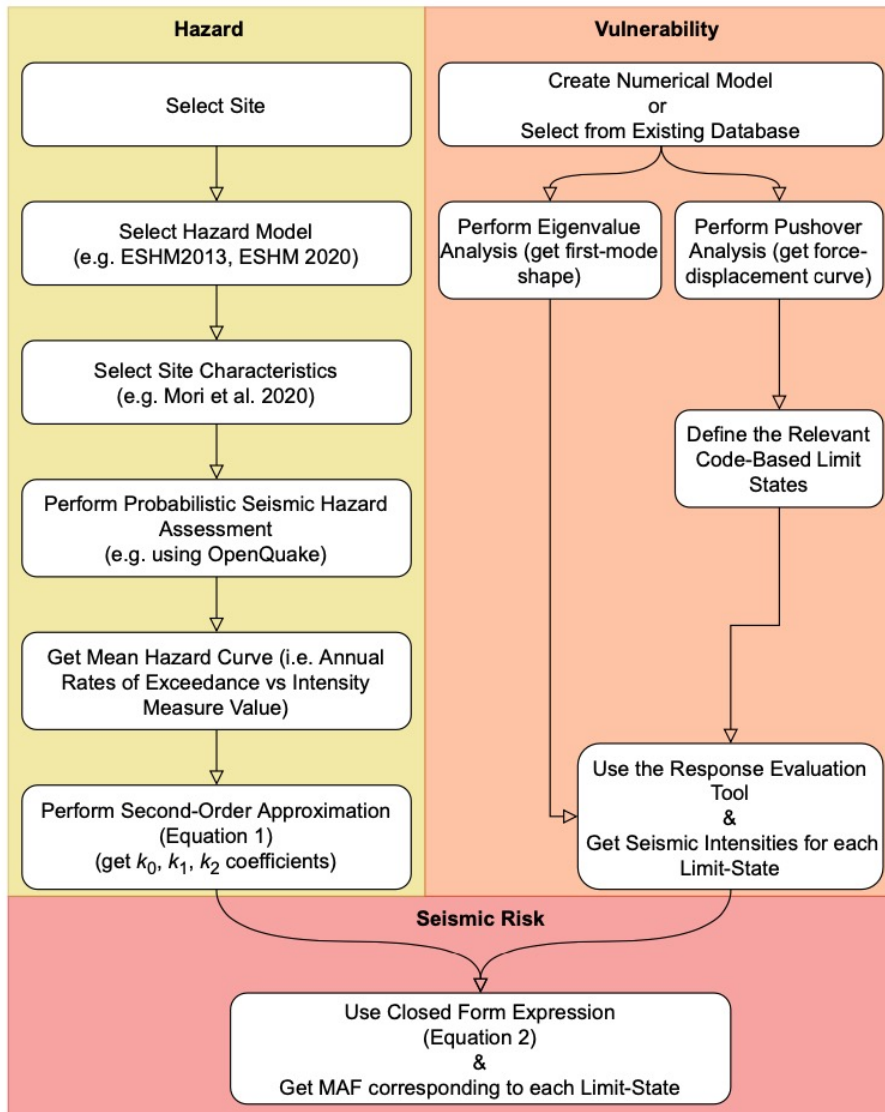
$$H(s) = k_0 \exp[-k_2 \ln^2(s) - k_1 \ln(s)] \quad (\text{Eq. 1})$$

where $H(s)$ is the hazard function and s is a given intensity measure value. k_0 , k_1 and k_2 are positive real numbers describing the curvature and amplitude of the hazard curve fit

Simplified Risk Estimation

ROSE Online Seminar

12th October 2022



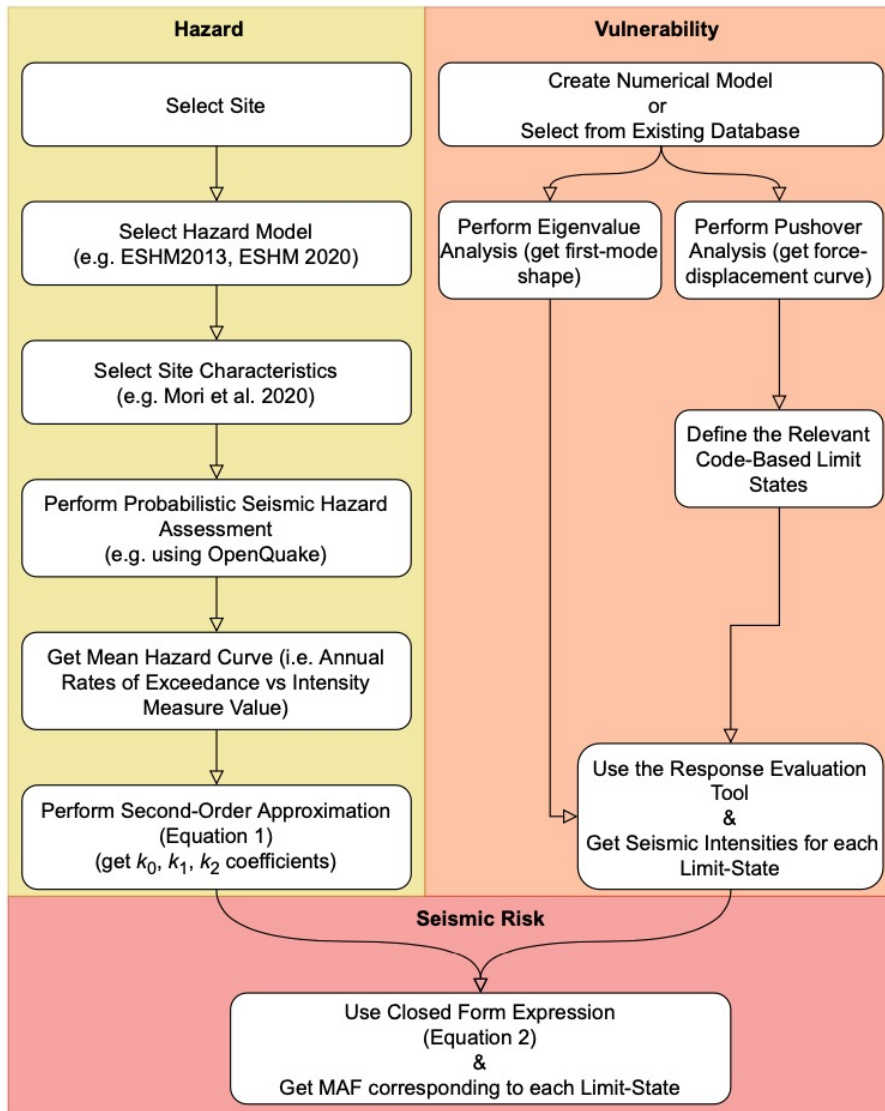
Vulnerability

1. Build numerical model
2. Perform eigenvalue analysis and get the first-mode shape ordinate (Φ_i) and mass (m_i) at floor i
3. Perform pushover analysis and get the nominal base shear force and roof displacement curve ($F-\Delta$)
4. Multilinearise the $F-\Delta$ curve
5. Define the code-based limit-states and annotate on the pushover curve
6. Use the response estimation tool to estimate the median seismic intensities and the associated dispersions

Simplified Risk Estimation

ROSE Online Seminar

12th October 2022



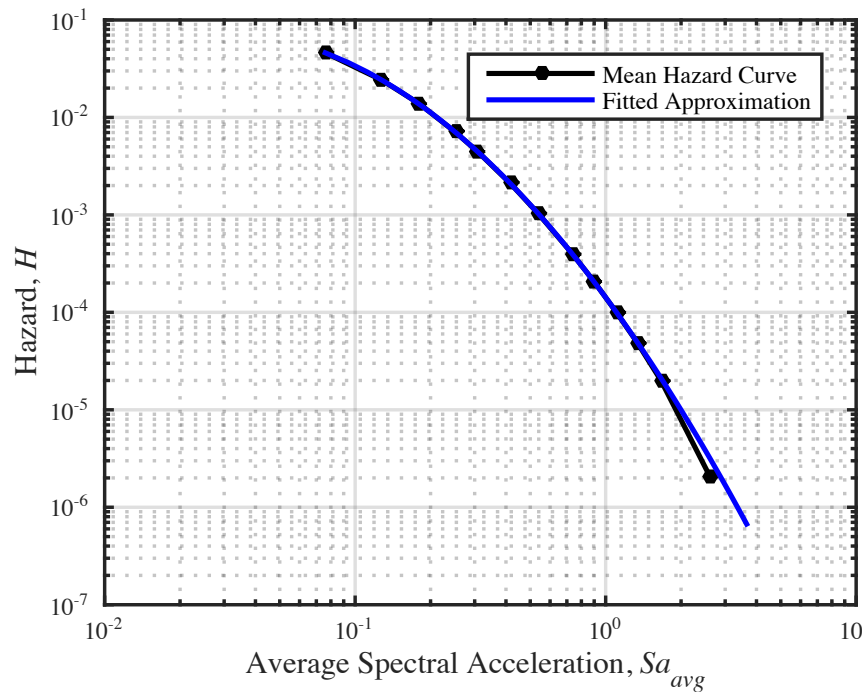
Seismic Risk

$$\lambda_{LS} = \sqrt{pk_0^{1-p}} [H(\hat{s}_c)]^p \exp\left[\frac{k_1^2}{4k_2}(1-p)\right] \quad (\text{Eq. 2})$$

$$p = \frac{1}{1+2k_2\beta^2} \quad (\text{Eq. 3})$$

where β corresponds to the record-to-record variability. $\beta = 0.27$ for non-collapse limit-states and 0.38 for the collapse limit-state and $H(\hat{s}_c)$ represents the annual rate of the median intensity measure required to attain a particular demand-based level

Example Application (Cont'd)



Mean hazard curve and fitted second-order polynomial for a site in Napoli, Italy.
The coefficients were found through a least-squares regression to be $k0=1.42e-04$, $k1=3.50$ and $k2=0.49$

Example Application

$$H(\widehat{Sa}_{avg,LS1}) = k_0 \exp[-k_2 \ln^2(\widehat{Sa}_{avg,LS1}) - k_1 \ln(\widehat{Sa}_{avg,LS1})] = (1.04E - 04) \exp[-0.49 \ln^2(0.31) - 3.50 \ln(0.31)] \\ = 0.044$$

$$p = \frac{1}{1 + 2k_2 \beta_{NC}^2} = \frac{1}{1 + 2(0.49)(0.27)^2} = 0.93$$

$$\lambda_{LS1} = \sqrt{p} k_0^{1-p} [H(\widehat{Sa}_{avg,LS1})]^2 \exp\left[\frac{k_1^2}{4k_2} (1-p)\right] = \sqrt{0.93}(1.42E - 04)^{1-0.93}[0.0044]^{0.93} \exp\left[\frac{3.50^2}{4(0.49)} (1-0.93)\right] \\ = 0.0051$$

Direction	Limit-State	\widehat{Sa}_{avg}	$H(\widehat{Sa}_{avg})$	β	p	λ_{LS}	$T_R = 1/\lambda_{LS}$ [Years]
X	LS1	0.31	0.0044	0.27	0.934	0.0051	195
	LS2	0.46	0.0016	0.27	0.934	0.0020	499
	Collapse	0.73	3.74e-04	0.38	0.876	6.75e-04	1481
Y	LS1	0.32	0.0044	0.27	0.934	0.0051	195
	LS2	0.49	0.0013	0.27	0.934	0.0017	498
	Collapse	0.75	3.91e-04	0.38	0.876	7.01e-04	1427

Summary of the simplified risk assessment results

Code-Based Application (Comparison with extensive NLTHA)

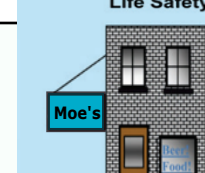
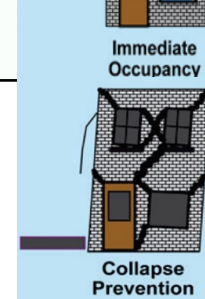
- a. Identification of code-based (i.e. NTC2018) limit states thresholds
- b. Simplified risk assessment using PB-Risk
- c. Extensive risk assessment using hazard-consistent records
- d. Comparison of results in terms of median seismic intensities and dispersion
- e. Comparison of results in terms of mean annual frequency of exceedance
- f. Comprehensive comparison with code-based non-linear static procedures (using a set of 40 archetype buildings)

Simplified Risk Estimation

ROSE Online Seminar

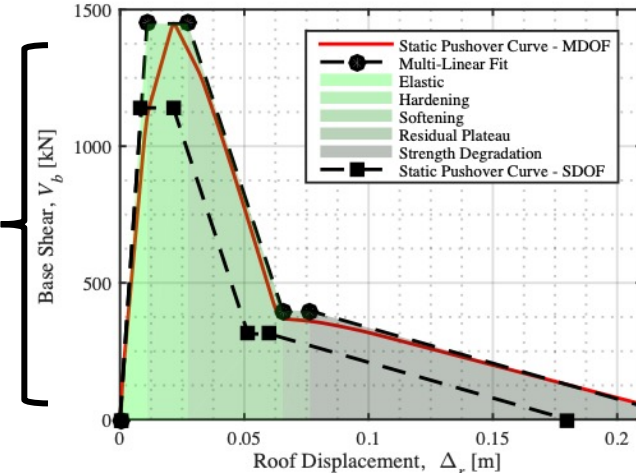
12th October 2022

a. Identification of limit-states thresholds

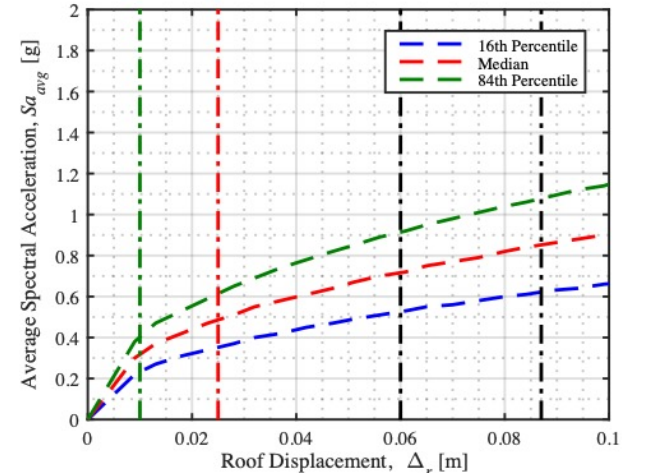
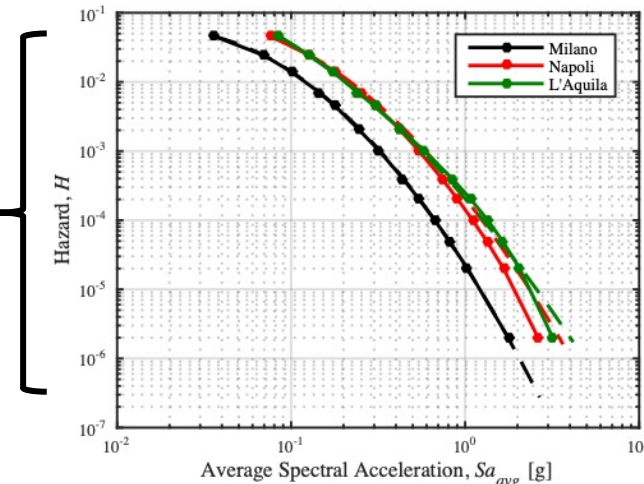
Limit-State	Description	Illustration
Stato Limite di Operatività 'Operational' (SLO)	Structural and non-structural elements maintain functionality without suffering damage and significant interruption of usage. Moderate damage to infill panels is foreseen at low levels of drift	
Stato Limite di Danno 'Damage Control' (SLD)	Structural and non-structural elements suffer moderate damage. Structure remains under immediate occupancy without jeopardizing human life. The overall capacity and stiffness of the structure is not compromised	
Stato Limite di salvaguardia della Vita 'Life Safety' (SLV)	Structure sustains heavy damage to its structural elements resulting in a significant loss of lateral stiffness. The structure retains its gravity load carrying capacity with a margin of safety against collapse. Failure of non-structural elements is a direct consequence of attaining SLV	
Stato Limite di prevenzione del Collasco 'Collapse Prevention' (SLC)	Structural and non-structural elements suffer heavy damage. The structure maintains gravity-load carrying capacity with a slender margin of safety against collapse due to the full exploitation of the strength and deformation capacity	

b. Simplified risk assessment using PB-Risk

Vulnerability

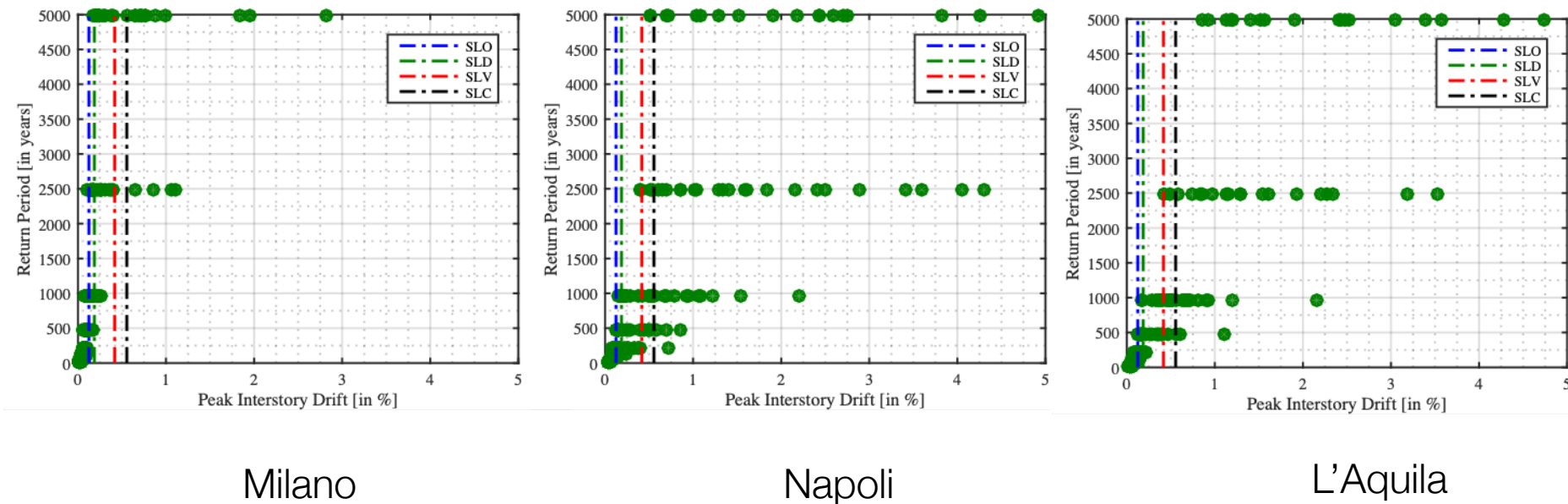


Hazard



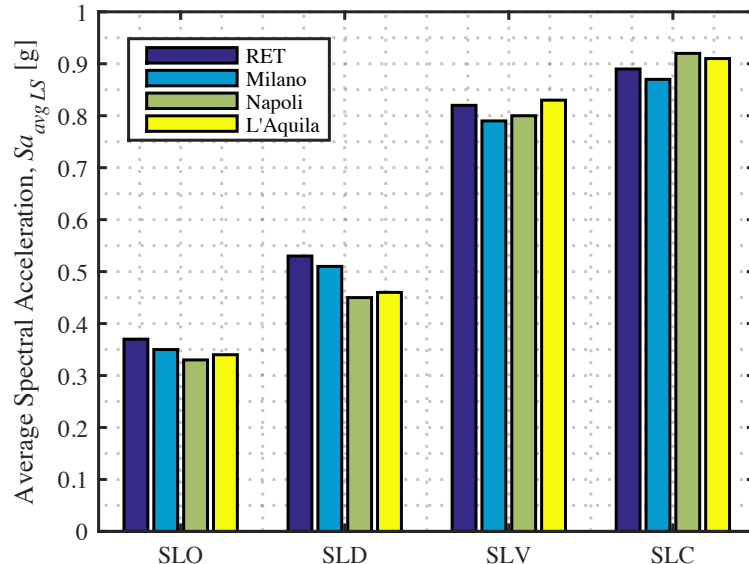
Site	Second-Order Approximation Coefficients		
	k_0	k_1	k_2
Milano	2.20e-05	3.95	0.50
Napoli	2.09e-05	3.20	0.43
L'Aquila	2.04e-05	2.92	0.29

c. Extensive risk assessment using hazard-consistent records

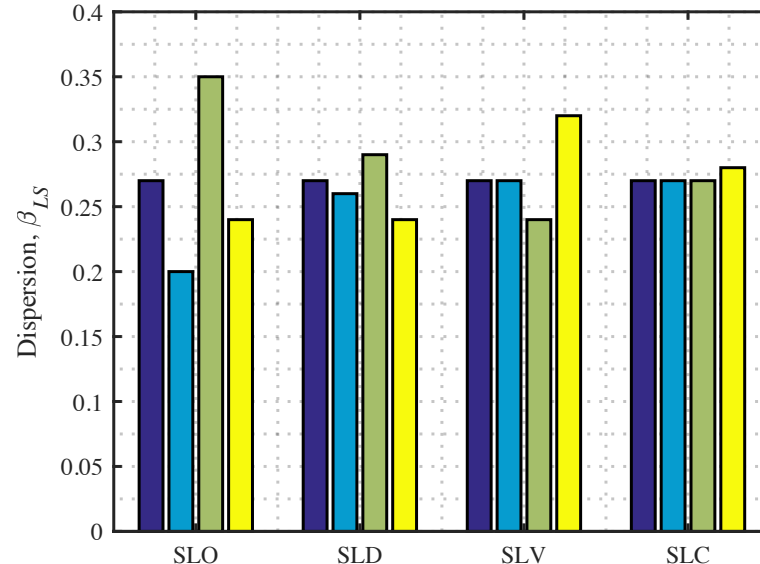


Multiple stripe analysis corresponding to nine return periods (22, 42, 72, 140, 224, 475, 975, 2475, 4975) and illustrating the structural response associated with increasing levels of ground motion intensity

d. Comparison of results in terms of median seismic intensities and dispersions



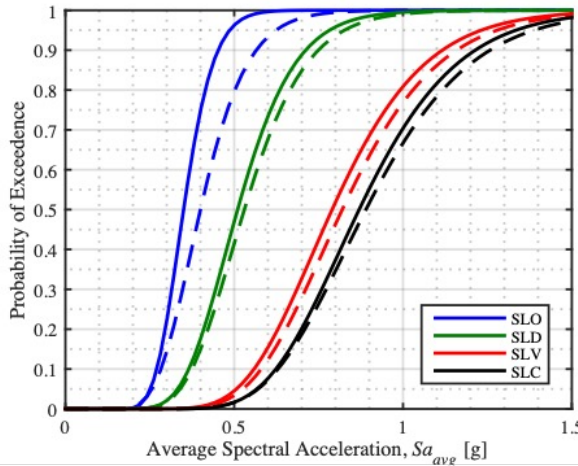
Median Seismic Intensities ($Sa_{avg,LS}$)



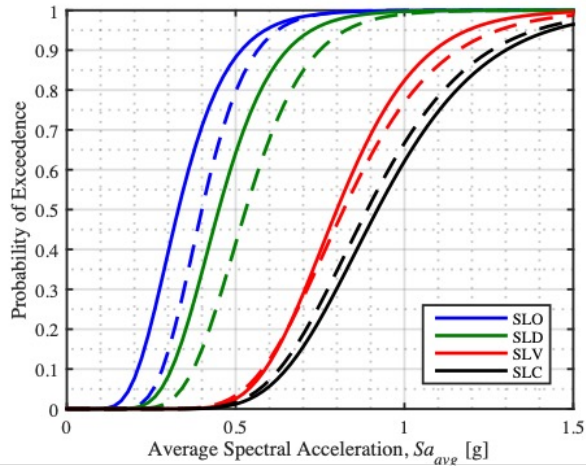
Record-to-Record Variability (β_{RTR})

Median seismic intensities and the associated record-to-record variability recorded at the three selected locations corresponding to the code-based limit-states and evaluated following NLTHA and the response evaluation tool (RET).

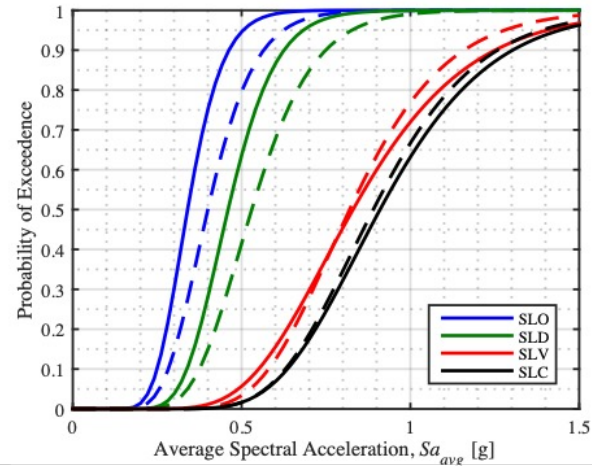
d. Comparison of results in terms of median seismic intensities and dispersions



Milano



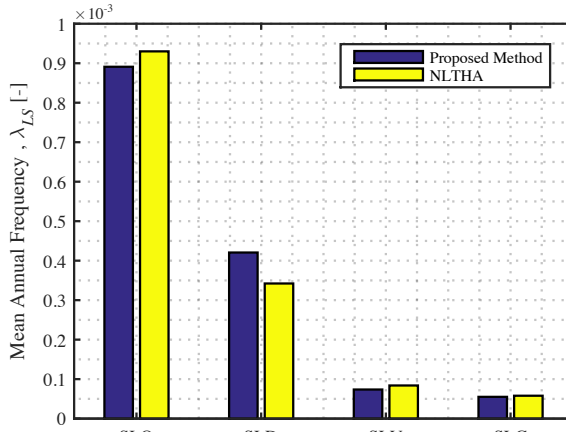
Napoli



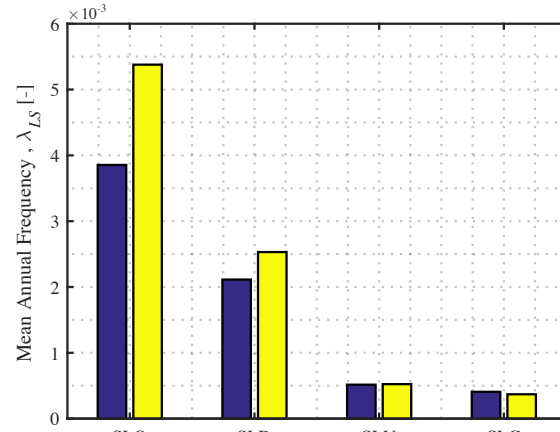
L'Aquila

Fragility functions recorded at the three selected locations corresponding to the code-based limit-states and evaluated following NLTHA (solid lines) and the response evaluation tool (dashed lines).

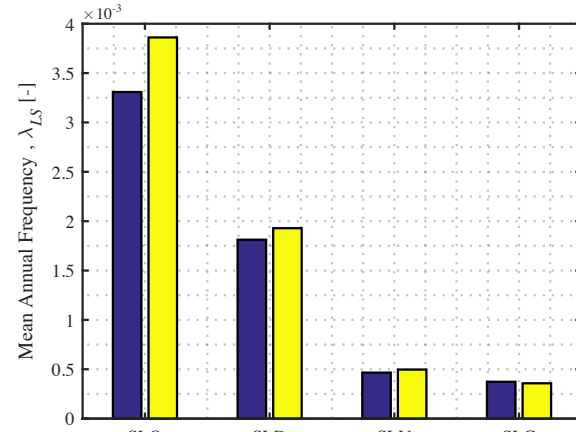
e. Comparison of results in terms of mean annual frequency of exceedance



Milano



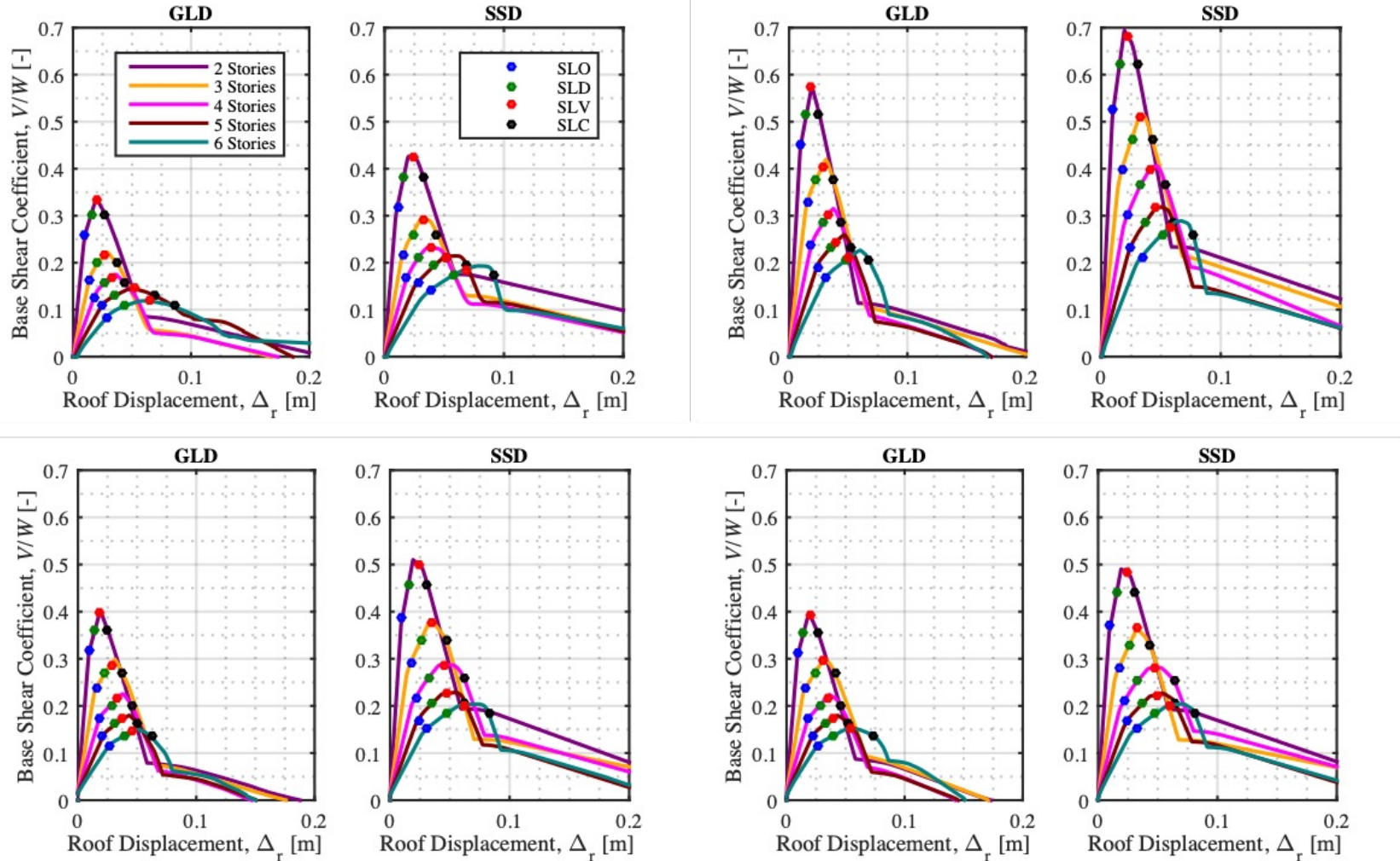
Napoli



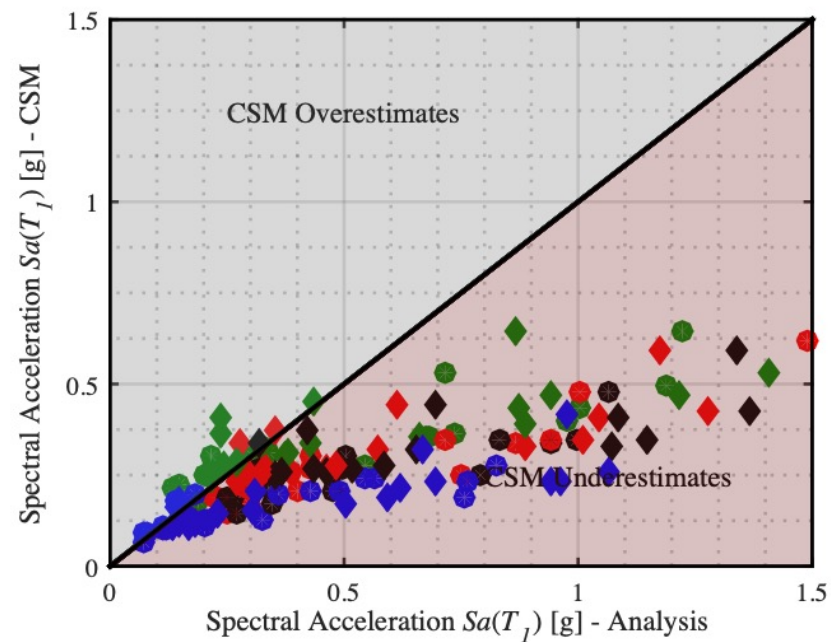
L'Aquila

Seismic risk estimates expressed in terms of the mean annual frequency of exceeding the demand- based thresholds corresponding to each limit state evaluated using detailed analysis and the proposed simplified method of assessment for Milano, Napoli and L'Aquila.

f. Comprehensive comparison (definition of case study buildings)

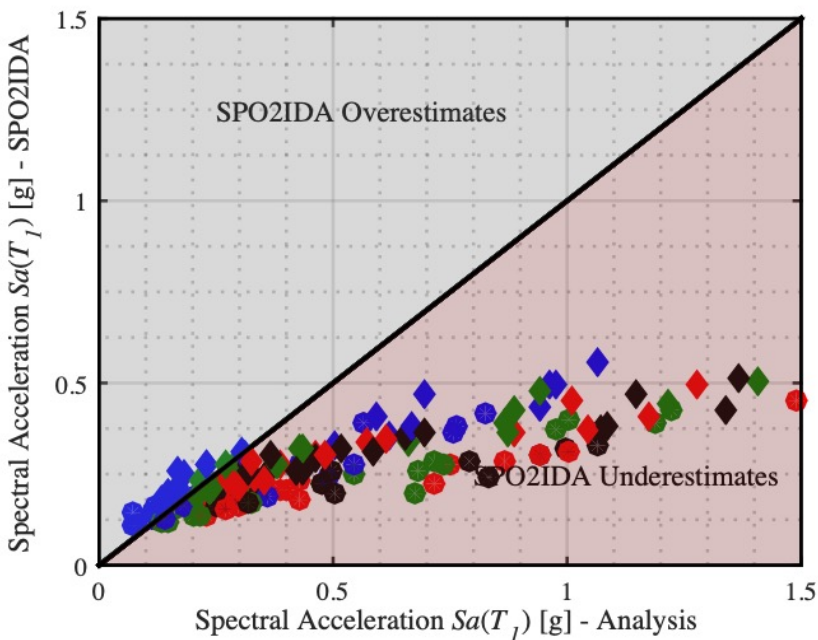


f. Comprehensive comparison (median intensities – capacity spectrum method)



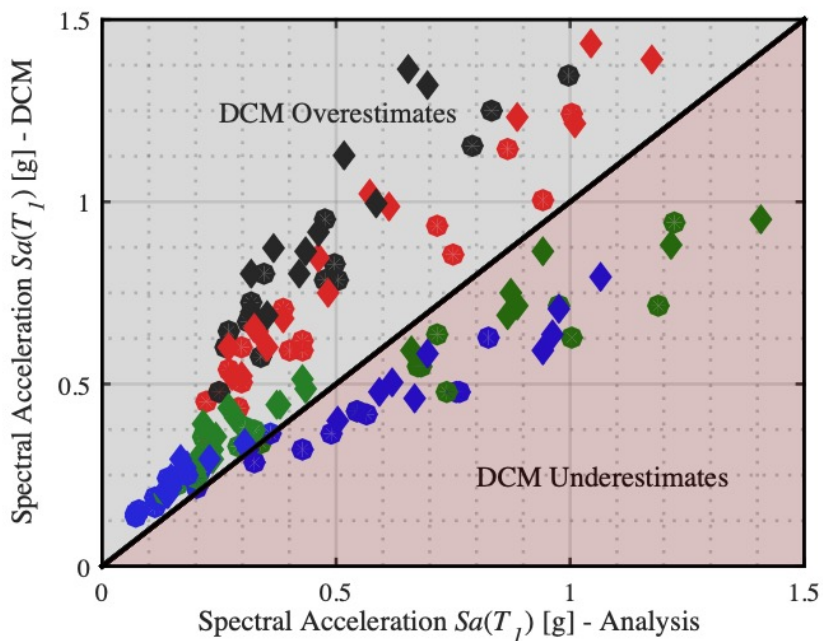
- Consistent underestimation of the seismic intensity with respect to NLTHA
- Drawbacks of CSM:
 - Relates the hysteretic energy dissipation of an inelastic system with an equivalent viscous damping model in an equivalent linear system, for highly inelastic systems
 - Traditional equivalent viscous damping model was developed for bare RC frame structures
 - Incompatibility with infilled RC frame structures due to the inherent higher damping in said typology
 - Non-convergence and underestimation of the actual seismic demand (i.e. a higher intensity is required to achieve a particular demand threshold)

f. Comprehensive Comparison (median intensities – SPO2IDA)



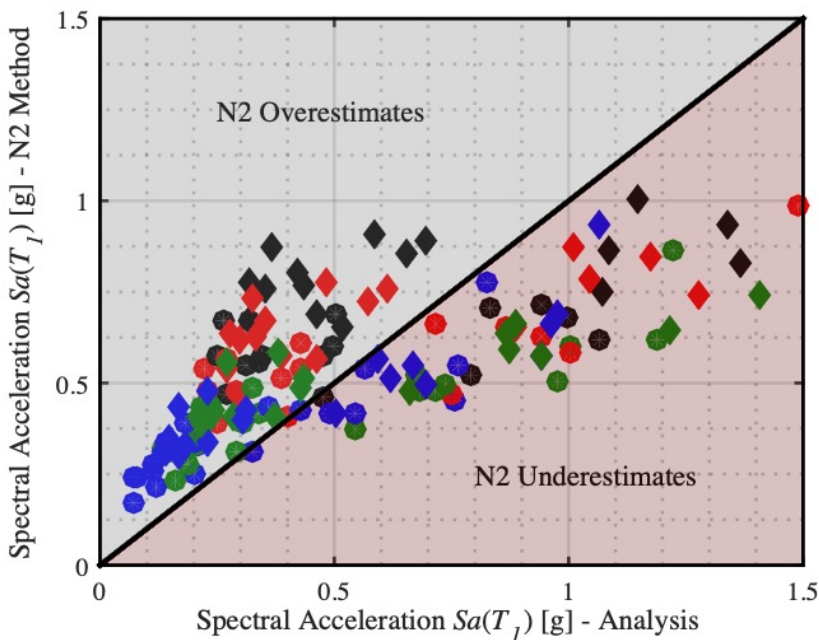
- Consistent underestimation of the median intensities with respect to NLTHA
- Drawbacks of SPO2IDA:
 - Fundamental difference in the behaviour of framed structures of different typologies
 - For systems modelled without masonry infills, first mode dominates the response and a simple bilinear hysteretic model is sufficient to capture the structural behaviour until collapse
 - For systems modelled with masonry infills, a period shift and a modification of the first mode behaviour is expected due to the premature exhaustion of the masonry infill capacity
 - Additional energy dissipation capacity of the infill renders this simplified method unable to accurately predict the capacity

f. *Comprehensive Comparison (median intensities – displacement coefficient method)*



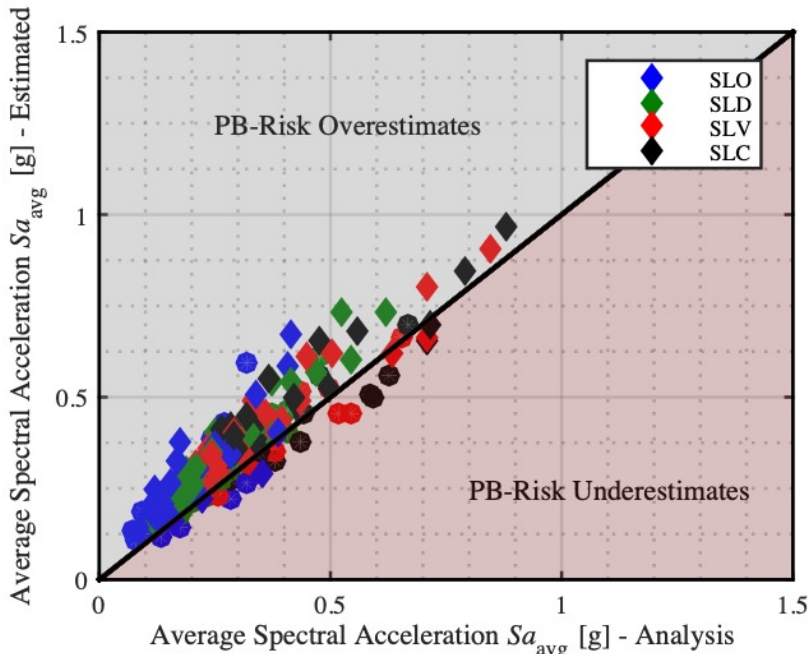
- Significant scatter and inconsistency around the median intensities with respect to NLTHA
- Drawbacks of DCM:
 - Relies on several coefficient to account for the general characteristics of the structural typology (not necessarily the specific structural behaviour)
 - Coefficients are determined for the expected displacement (elastic and inelastic) ratio for a bilinear SDOF systems, effects of the pinching in-load deformation relationships due to stiffness and strength degradation, second-order geometric non-linearities
 - Coefficients are calibrated for SDOFs with non-evolutionary hysteretic relationships
 - FEMA guidelines highlight potential errors for systems with $T < 0.4s$

f. Comprehensive Comparison (median intensities – N2 Method)



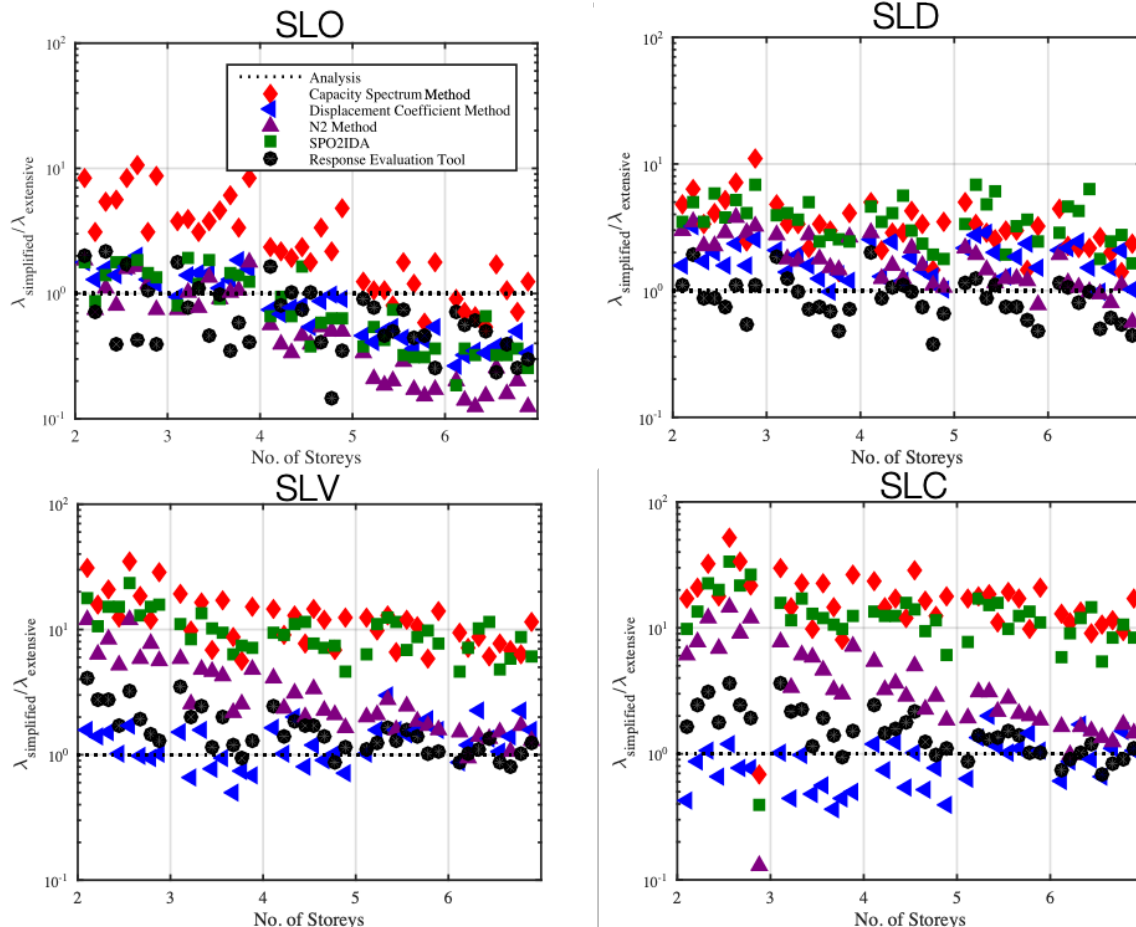
- A relatively good match and low scatter at all lower LSs and underestimation at higher LSs
- Drawbacks of N2 Method:
 - Limitations in the $R-\mu-T$ relationships
 - Choice of IM ($Sa(T_1)$)
 - Range of parameters defining the idealized pushover curve
 - In the medium and long period ranges, the assumptions made are valid such as: the equal displacement rule, the reduction factor R_μ is relatively constant for different sets of accelerograms
 - In the short period range, the sensitivity of inelastic displacements to changes of structural parameters is greater, therefore estimates are inaccurate

f. Comprehensive Comparison (median intensities – PB-Risk)



- A relatively good match and low scatter across all LSs
- Benefits of PB-Risk:
 - Adequate characterization of the structural response using representative infilled RC SDOF oscillators
 - The use of the average spectral acceleration as opposed to the spectral acceleration at the fundamental period, accounting for the period elongation effects and reducing the record-to-record variability
 - The reduction of bias influencing the structural response due to the scaling of ground-motions with the adoption of cloud analyses

f. Comprehensive comparison (risk estimates)



- Risk estimates of existing NSPs exhibited similar conservativeness with an overestimation of seismic risk compared to the benchmark risk values from NTLHA.
- PB-Risk demonstrated consistent results and a higher correlation to the same benchmark values.
- Conservativeness is more appealing for carrying-out design and assessment studies where safety margins are necessary
- Accuracy and consistency are arguably more desirable within a broader financial loss assessment setting, which the PB-Risk has been shown to offer.

Conclusions

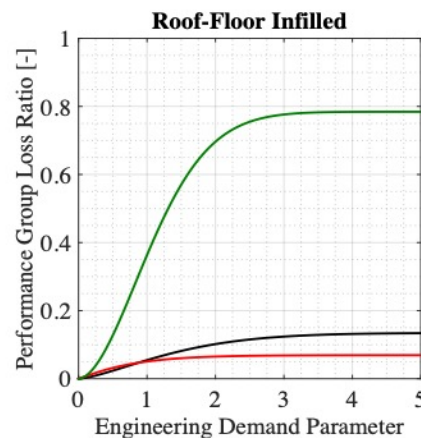
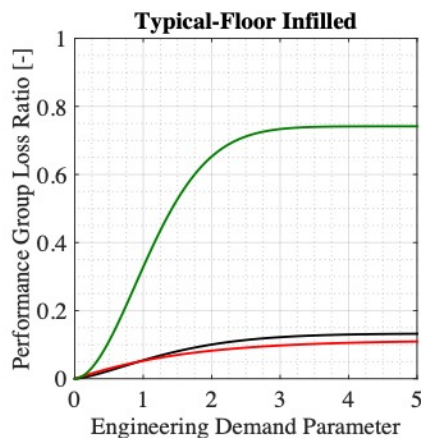
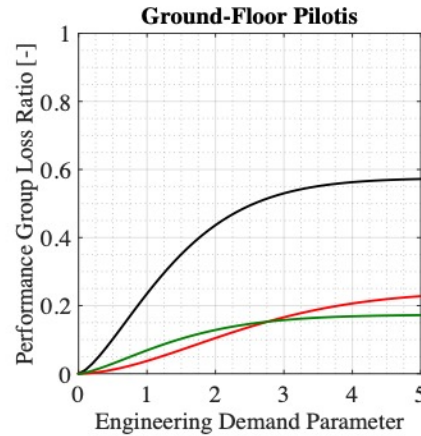
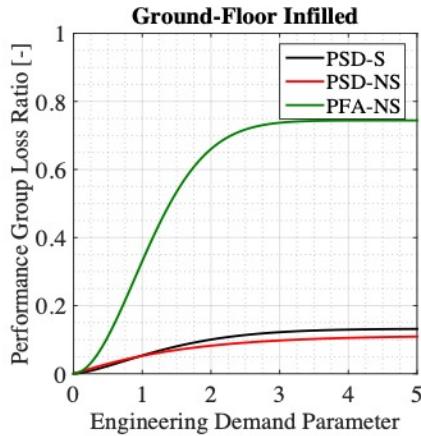
- A methodology was presented for the simplified pushover-based seismic risk assessment of non-ductile infilled RC frame buildings.
- The method relies on a second-order power-law fit for the characterisation of seismic hazard
- The method a pushover-based response estimation tool for the fast evaluation of empirical strength-ductility relationships to quantify their seismic vulnerability
- The method considers the SAC/FEMA closed-form expressions to estimate mean annual frequency of limit-state exceedance for risk-based applications.
- The results of PB-Risk highlighted the reliability, consistency and reproducibility rendering it a potential improvement to be implemented in risk classification guidelines such as Sismabonus in Italy, specifically for the infilled RC typology



Current Research

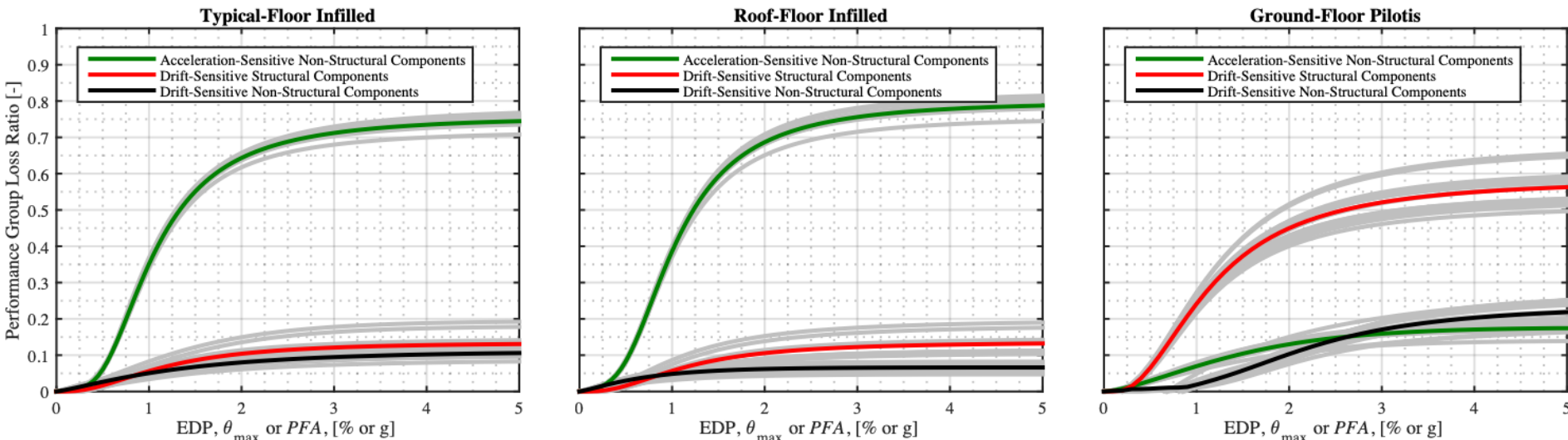
Simplified approach for the loss assessment of existing structures using generic storey-loss functions

Proposed Approach



- Generic set of storey-loss function for the estimation of economic losses tailored for infilled RC frame buildings
- Demand-based (i.e. storey drifts, peak floor acceleration) calibration of the expected loss ratios
- Consideration of typical damageable inventory (i.e. drift sensitive and acceleration sensitive components)
- Consideration of typical storey typologies (i.e. ground floor infilled, pilotis floors, typical infilled floors and roof floors)

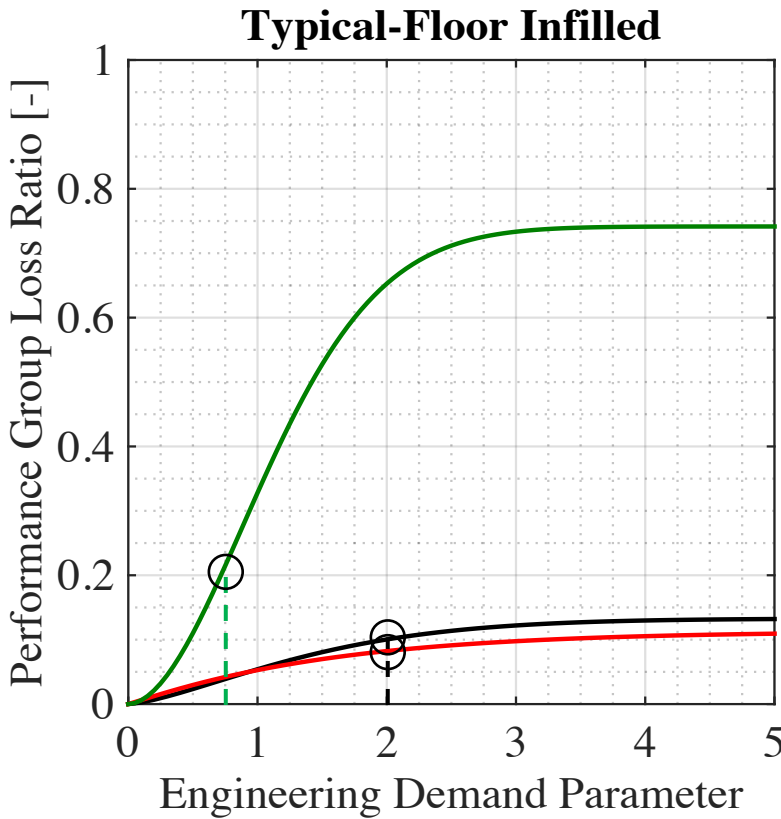
Calibration of Simplified Approach



Generic set of storey-loss functions for the simplified loss assessment of infilled, pilotis and roof floor typologies considering typical damageable inventory corresponding to the construction/architectural practice of the southern Mediterranean infilled RC building stock

- Shahnazaryan D, O'Reilly GJ, Monteiro R. Story loss functions for seismic design and assessment: Development of tools and application. *Earthquake Spectra*. 2021;37(4):2813-2839. doi:[10.1177/87552930211023523](https://doi.org/10.1177/87552930211023523)

Proposed Approach



- For each storey:

1. Determine the demands corresponding to the limit-state of interest using the RET
2. Depending on the floor typology, interpolate the corresponding loss ratio associated with drift and acceleration sensitive components
3. Sum the losses associated to damageable components at that particular limit state

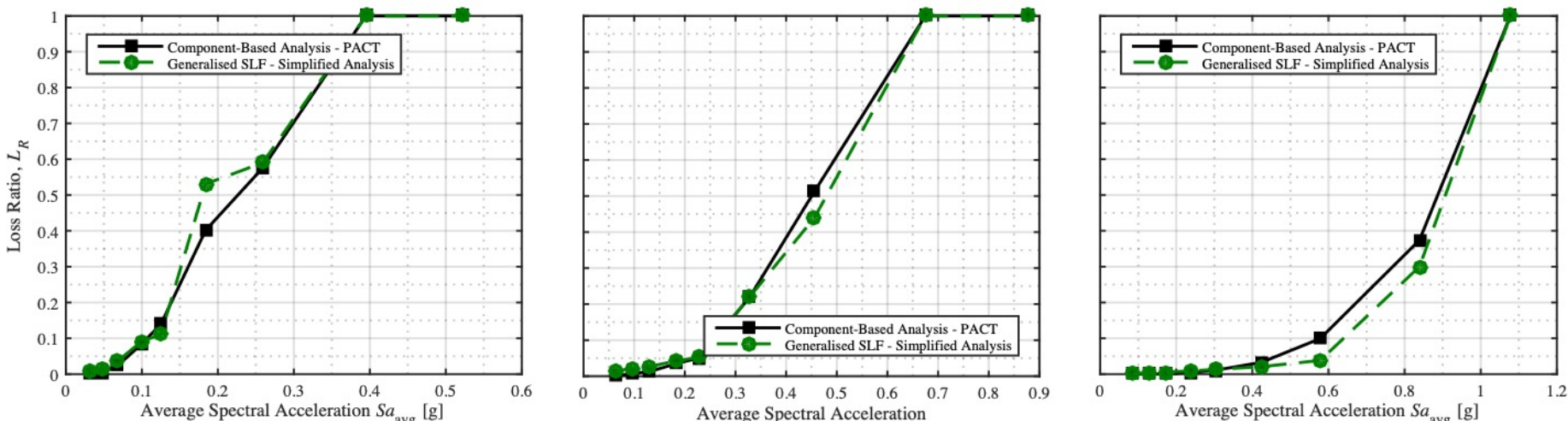
$$L_{R,LS,i} = L_{R,\theta-SC,i} + L_{R,\theta-NSC,i} + L_{R,PFA-NSC,i}$$

- The total loss is then determined as such:

$$TL_{R,LS} = \sum L_{R,LS,i}$$

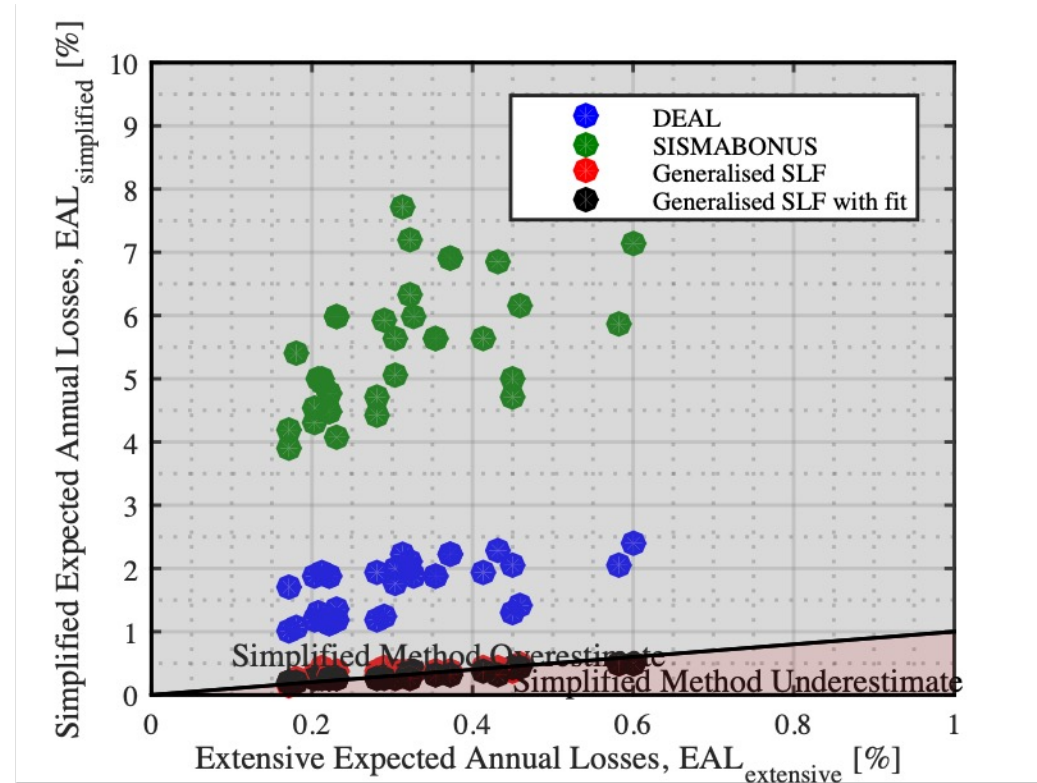
- Calvi PM, Sullivan TJ. Estimating floor spectra in multiple degree of freedom systems. *Earthq Struct.* 2014;7(1):17-38.
- Vukobratović V, Fajfar P. A method for the direct estimation of floor acceleration spectra for elastic and inelastic MDOF structures. *Earthq Eng Struct Dynam.* 2016;45:2495-2511.

Application to one-storey buildings



Vulnerability curve (loss ratio versus intensity measure) corresponding to single-storey pilotis floor typology (left); typical infilled floor (center); roof typology (right)

Application to GLD case study structures



Expected annual loss values corresponding to various simplified methods (i.e. DEAL, SISMABONUS, Generalised SLFs) in comparison with the extensive component-based approach through PACT

Thank you for your attendance

e-mail: mouayed.nafeh@iusspavia.it

